Authors' response: Batenburg et al., 2016

Detailed response to the reviews

The reviewers' comments are copied in grey, our original response in black, and the applied changes are indicated in blue. Page and line numbers in blue refer to the revised manuscript. The replies are followed by a list of relevant changes and a marked-up version of the manuscript.

Reviewer #1

1. Does the paper address relevant scientific questions within the scope of CP? Yes, the authors want to show and explain climate control on the development of poor oxygenation conditions in the ocean during the Late Cretaceous.
2. Does the paper present novel concepts, ideas, tools, or data? This paper doesn't really present any new ideas, but it has many new data and a slightly different approach from previous papers on the same subject. This paper attempts to define the time frame of the Cenomanian-Turonian interval by integrating new radiochronologic data and using more recent astronomical data. Cyclostratigraphic analysis is performed on data in part different than previously.
3. Are substantial conclusions reached? No, because this article does not stand out enough from that of Mitchell et al., 2008 and the differences in interpretation are not sufficiently justified.

We are happy to read that the reviewer recognizes the significant amount of new paleoclimate proxy data that is presented in our manuscript, as well as a new radioisotopic date for the Cenomanian. Still, the reviewer has the opinion that that our manuscript does not stand out enough from Mitchell et al. (2008). In the original version of the manuscript, we have listed a number of differences in tuning approach and interpretation between Mitchell et al. (2008) and our manuscript. One important difference is that we solely use the stable 405 kyr periodicity of eccentricity as a tuning target, whereas Mitchell et al. (2008) also tuned to 100-kyr eccentricity. We adopt this tuning strategy because the 405-kyr component is the only astronomical tuning target that can be used beyond ~50 Ma, and is thus the prime target in the Mesozoic. The C/T boundary age might seem similar between the two papers, but this is in fact not the case. Mitchell et al. (2008) used radioisotopic ages of Sageman et al. (2006), who used the Fish Canyon sanidine standard age of 28.02 ± 0.28 Ma of Renne et al. (1998), while we use the 28.201 ± 0.046 Ma of Kuiper et al. (2008). At around 94 Ma, this makes a difference of more than 600 kyr or 1.5 x 405-kyr cycle. This improvement is critical for extending the astronomical time scale from the K/Pg boundary back to the C/T boundary and beyond.
The discussion of differences in approach between Mitchell et al. (2008) and our paper, however, did not seem to be effective in indicating the fundamental differences that exists between both works. Therefore, we recognize that this part of the manuscript should be improved. In the revised version of the manuscript, we are paying special attention to the discussion of the differences in cyclostratigraphic approach and paleoenvironmental interpretation between Mitchell et al. (2008) and Batenburg et al. (2016). This involves a fundamental rewriting of the paragraphs involved.

We include a new paragraph on page 11 (l.10–17) summarising the new aspects of our study, including 1) the use of only the 405-kyr periodicity component of eccentricity from the new La2011 solution, 2) the independent estimate of the duration of deposition of the Livello Bonarelli, 3) the consequences of the use of the new intercalibrated age of the Fish Canyon sanidine and 4) the new radioisotopic age of the mid-Cenomanian event. Points 1) and 3) are particularly relevant in comparison to the Mitchell et al. (2008) study, and are discussed further on page 11, l. 18–25 and page 13, l. 4–11, respectively.
In addition, on page 16, lines 16–21 explain the difference in invoked climatic mechanisms between Mitchell et al. (2008) and the present study.

4. Are the scientific methods and assumptions valid and clearly outlined? More or less The assumptions seem to be more or less valid, but there are too many assumptions. For example: - The correlation between MS et chert ; - The link between the different proxies studied and the carbon cycle - The contribution of nutrients from Caribbean plateau activity. One may ask how the transfer of material in view of the cenomanian paleogeographic configuration is. I think, as

authors, both the climate and the Caribbean plateau activity are at the origin of the Cenomanian-Turonian anoxic nevertheless this paper does not really show it.

Figure 3 shows the relationship between MS and cherts, as well as the relation with different proxies. The link between this study and the long-term behavior of the carbon cycle is discussed in paragraph 4.4, as is the likely supply of nutrients from the Caribbean LIP. Volcanism was probably the ultimate driver of oceanic anoxia, but, based on our findings, astronomical forcing likely determined the exact timing. We focus on the astronomical forcing aspect and consider the precise oceanographic processes and geochemical pathways beyond the scope of this paper.

In section 4.3.1 (p.14) on the expression of long-term eccentricity forcing, we explain the patterns observed in the lithology and the carbon isotope data that are indicative of the behaviour of the 2.4 Myr cycle of eccentricity in more detail. We have also revised the following section on the relation with volcanism (4.3.2, p. 15-16) to include more specific information on previously published studies on volcanic activity and ocean circulation during the Cenomanian–Turonian transition to put our findings in a larger context.

5. Are the results sufficient to support the interpretations and conclusions? No

5.1 Because there is no discussion on the choice and the climatic significance of the different proxies studied. Why do studied proxies differ according to stratigraphic interval? Unfortunately these proxies do not have the same meaning: The reflectance is controlled by the lithology. The SiO2 concentration is function of both detrital influx variations and authigenic / biogenic silica content. The concentration of Al2O3 and TiO2 reflects changes in detrital flow. Magnetic Susceptibility (MS) variations are function of the concentration in dia-, para and ferromagnetic minerals. How do you explain the increase in MS in levels rich in diamagnetic minerals? Is it strange? Have you done a statistical analysis which shows the correlation between MS and authigenic/ biogenic SiO2 content?

Different paleo-environmental proxies have been measured between the Scaglia Rossa/Bianca Formations on the one hand (C and O stable isotopes, magnetic susceptibility, reflectivity and limestone-chert alternations), and the Livello Bonarelli on the other hand (XRF-derived SiO_2, Al_2O_3, TiO_2 and Loss-on-Ignition). The large differences in sedimentary facies imply that different proxy records form the best archives for paleoclimatic variability. For example, reflectance data are very useful in the interval where black shales occur, whereas colour variations in the Scaglia Bianca (above the Livello Bonarelli) are limited. We discuss the characteristics of the different proxies in terms of paleoclimatic and paleo-environmental interpretation in more detail in the revised version of the manuscript. As the individual proxy records are limited to the lithological units, we do not have overlapping magnetic susceptibility and SiO_2 data, and cannot perform statistical analyses.

The choice and significance of the proxies is now discussed more thoroughly in section 2.1 (Geological setting and proxy records), in particular on page 4, lines 13–25, and in section 4.1 (Proxy records and correlation of the C/T boundary) from page 8, line 21 to page 9, line 9.

5.2 How did you measure the δ13 C in chert? These analyzes do not explain what is the minimum carbonate content for valid δ13 C values?

$\delta^{13}C$ values were obtained from powdered samples, of the limestones and marls as well as of the cherts, which still contained carbonate. If, in the first measurement run, carbonate concentrations were too low to obtain a reliable signal, measurements were repeated with a larger volume. This information is being incorporated in the revised manuscript.

This information is inserted on page 5, lines 3–4.

5.3 The authors state “we procure insights in the relationship between orbital forcing and the ´ Late Cretaceous carbone cycle by deciphering the imprint of astronomical cycles on lithologic, geophysical and stable isotope records. . . “ but the data shows that the imprint of astronomical cycles in the stable isotope records and specially δ13C is very difficult for deciphering, that’s why, the cyclostratigraphic analysis is applied to others proxies whose link with the carbon cycle is not shown.

The cyclostratigraphic framework is indeed constructed based primarily on the geophysical proxies and the limestone-chert alternations. In Figure 2, we show that eccentricity maxima, as interpreted from these proxies, correspond to high variability in $\delta^{13}C$, as well as with a tendency towards more negative $\delta^{13}C$ values. This is one example of how we link the cyclostratigraphic interpretations with the global carbon cycle. Additionally, one of the significant findings reported in this manuscript, is the fact that the base of the Livello Bonarelli corresponds to the first 100-kyr eccentricity maximum after a 405-kyr eccentricity minimum, which is another clear example of a link between cyclostratigraphy and global carbon cycle perturbations.

The construction of our cyclostratigraphic framework is discussed in more detail in section 4.2.2 (Calibration to 405-kyr eccentricity), on page 11, lines 4–25.

> Some authors' conclusions are in agreement with Mitchell et al. (2008) works. Mitchell et al. in particular, show a cyclicity of about 2.4 Ma in the development of anoxia. Unlike Mitchell's works Batenburg et al. suggest that "the exact timing of major carbon cycle perturbations during the Cretaceous may be linked to increased variability in seasonality partner after the prolonged avoidance of seasonal extreme" at the 2.4 Myr scale. This interpretation is not confirmed on any figure. We don't see the 2.4 Myr cycles on Figure 3.

A possible role of the 2.4 Myr eccentricity cycle is discussed after the observation that the mid-Cenomanian event, the OAE-2 and the Pewsey excursion are separated by 2.0 - 2.4 Myr respectively, and the observation that black shales are lacking in the interval preceding OAE2. This lithological pattern and the spacing between the three "events" can be observed in Figure 3.

Sections 4.3.1 and 4.3.2 (pages 14–16) discuss the observations on the influence of the 2.4 Myr periodicity of eccentricity in more detail, as well as the effects of the suggested particular orbital configuration on climate and oceanography.

> Why are not the insolation variations calculated from La2011 data presented?

This is because the most recent insolation solution that is currently available is La2004. This insolation solution is only valid until ~40 Ma. The La2011 and La2010 solutions that are available at present, are eccentricity-only solutions. Only the 405-kyr eccentricity component of the La2010 and La2011 solutions can be used in the Cenomanian/Turonian interval.

6. Is the description of experiments and calculations sufficiently complete and precise to allow their reproduction by fellow scientists (traceability of results)? Yes, but scientific reasoning should be more explicit

We agree with the reviewer that scientific reasoning should be more straight-forward and explicit in the revised version of the manuscript. Therewith, we first and foremost focus on [1] showing the differences with the Mitchell et al. (2008) approach and [2] the hypothesis that OAE2 was favored by a specific sequence of astronomical configurations, with a prolonged period of low eccentricity (2.4 Myr eccentricity minimum) followed by an eccentricity maximum (100-kyr eccentricity maximum).

We have thoroughly revised the Discussion sections (see comments in blue above).

7. Do the authors give proper credit to related work and clearly indicate their own new/original contribution? I don't doubt the quality of the data, but the choice of these data should be better explained. Their own new contribution is clearly indicated.
8.
9. Does the title clearly reflect the contents of the paper? With this title and content, this article does not stand out enough of Mitchell et al. (2008) works.

See above.

10. Does the abstract provide a concise and complete summary? Yes
11. Is the overall presentation well structured and clear? I think the section "results" requires a total reorganization. Before addressing the proxy data and the link with the lithology, we should discuss the time frame of these series (radioisotopic dating + correlation). Any cyclostratigraphic

analysis must begin with an accurate (bio)chronological framework. The authors indicate, correctly, that the stratigraphic timing is not based on biostratigraphic, but chemostratigraphic correlations with well-dated series. I believe in the validity of such correlation, but nevertheless to valid a correlation, two continuous chemostratigraphic records must be correlated, which is not the case in this work (see Figure 9). Figure 9 is not convincing and not valid since it lacks isotopic data of the Bonarelli level. On the other hand, this figure is misplaced. It should be positioned at the beginning of the article. Thus, a part of the results and some figures should be reorganized. Another figure that shows the link between δ 13C and 2.4 kyr orbital cyclicity should be integrated.

We do not agree with the reviewer that our manuscript needs a total reorganization. The reviewer rightfully says that *"any cyclostratigraphic analysis must begin with an accurate (bio)chronological framework*". It goes without saying that we agree with this statement. Hence, the well-studied and well-documented biostratigraphic framework is presented early in the manuscript, in Figure 3, alongside the lithological column. Unfortunately, the reviewer misinterpreted our Figure 9, as this figure is not meant to constrain the initial stratigraphic framework by correlating outstanding features in d13C. Instead, Figure 9 shows a chemostratigraphic comparison between carbon isotope records from contemporaneous sections. In this figure, we show carbon isotope records along their original age-models, as constructed by the authors of the publications in which these data have been presented. In other words, Figure 9 is a figure in which we evaluate our tuning, and therefore, it should be presented after we presented the two tuning options for the studied sections. It is likely that the confusion was caused by the early call-out to Figure 9 in the original manuscript (Section 4.1), before the actual tuning is presented. In the revised version of the manuscript we discuss Figure 9 *after* we presented our tuning options for the studied sections.

The independent time constraints are now discussed more explicitly in section 4.2.3 (Integration with radioisotopic ages) in addition to the correlation of the C/T boundary (page 9, lines 10–22).

12. Is the language fluent and precise? Yes
13. Are mathematical formulae, symbols, abbreviations, and units correctly defined and used? Yes
14. Should any parts of the paper (text, formulae, figures, tables) be clarified, reduced, combined, or eliminated? Yes, In "Geological setting and proxy records" paragraph, the choice of proxies studied and their meanings must be explained. The "result" paragraph must be reorganized. Correlations and 2.4 kyr orbital cyclicity must be better argued. The modified Figure 9 should be placed at the beginning of the Article. The synthetic Figure 2 should be placed at end of the article.

These comments have all been addressed above.

15. Are the number and quality of references appropriate? Yes, but it is necessary to include additional references to explain the significance of the studied proxies
16. Is the amount and quality of supplementary material appropriate? There are not any

J. Laurin

Dear authors,
Congratulations on excellent data and an interesting paper. This study is an important contribution, although it might benefit from a better explanation of your approach to astronomical tuning. Could you please comment on the following points?

Published studies (Mitchell et al. 2008; Lanci et al. 2010) suggest relatively uniform sedimentation rates throughout the Furlo section (except of the Bonarelli L.). Your tuning options 1 and 2 imply markedly increased sedimentation rates (or reduced compaction) in the uppermost ~3 m beneath the Bonarelli Level (from ~1 cm/kyr to approximately 1.5 cm/kyr) and results in a ~100 kyr difference relative to the published age models. I realize that this part of the Furlo section is particularly difficult to interpret. Your L* data look great, and after examining your figures in detail I believe your age model might be correct (the apparent increase in both spacing and thicknesses of organic-rich beds in this interval are consistent with your interpretation). As it is, however, your tuning in this interval does not look very convincing. In section 3.3, lines 20-21 you explain that the identification of 405-kyr maxima and minima is based on a 3-5 m bandpass of L* data at Furlo. In both tuning options, however, the uppermost bandpassed maximum below the Bonarelli Level is out-of-phase relative to the 405-kyr maximum in La2011 to which it is correlated. You are apparently using other criteria, but they are not explained. I assume the correlation is based on the bundling of organic-rich beds. This aspect is, however, also problematic, because your lithological log for this interval shows important differences from L*, and it is not clear which of these two is used to define the bundles. For example, the circumflex that should mark the uppermost organic-rich bundle beneath the Bonarelli Level is centered at an exceptionally thick limestone in the lithological log (Fig. 3); this seems to contradict the definition of organic-rich bundles. It would be very helpful if you could show the detail of this part of the section and comment on the differences between your lithological log and color reflectance data. This is particularly important considering the disagreement between your interpretation and published age models.

We apologise for the lack of clarity in the tuning of the beds directly underlying the Livello Bonarelli. As this interval is at the edge of the band-pass filter, we prefer to base our tuning on the lithological pattern. The spacing of dark beds is in agreement with the reflectance record, and shows a bundle with thicker cherts and limestones. However, the use of circumflexes to indicate bundles and 100 kyr eccentricity maxima is unclear and introduces some ambiguity. In a revised version of the manuscript, we restrain from using circumflexes. Instead, we use brackets such as "}" spanning whole bundles and their centres as interpreted 100 kyr eccentricity maxima, and we discuss this specific interval in more detail.

Figure 2 has been adjusted, and the interval below the Livello Bonarelli is discussed on page 6, lines 18–22, as well as on page 14, lines 13–21.

Could you please explain why do you prefer tuning option #1 over tuning #2? I believe you have good reasons. Without an explanation (which I cannot find in your manuscript), however, the reader is puzzled especially when considering that your tuning #1 appears incompatible with some of the published radioisotopic/astrochronological estimates for the age of the C/T boundary (cf. Eldrett et al. 2015).

Tuning option #1 is in best agreement with the radioisotopic age for the Mid-Cenomanian event, presented in this study, and the intercalibrated ages for "Ash A" at the base of the *Whiteinella archaeocretacea* zone and the Cenomanian-Turonian boundary. However, tuning #2 is in better agreement with the recently published age of the C/T boundary of Eldrett et al. (2015). Based on our data, we cannot exclude either tuning option, but we discuss the differences with other timescales in more detail.

We have included a paragraph (page 13, lines 25–30) comparing the tuning options to radioisotopic ages and previous studies.

Your argument for a Myr eccentricity node prior to OAE II is based on the observed gap in the black shale occurrence at 483-485 m (page 8, lines 30-31). According to your tuning options, however, this interval experienced a 50-60% increase in sedimentation rates (or decrease in compaction) compared to the rest of the section beneath BL. If you apply correction for this change in sedimentation rate,

then the thickness of the shale-free interval decreases by c. 35 %. Such a correction would make this interval comparable to other 405-kyr minima in this section (e.g., ~471-472 m) and disqualify the argument for a Myr node. The exceptional thickness of dark levels above this interval (page 8, lines 31-32) can be attributed to the overall increase in (compacted) sedimentation rates as well.

When applying such a correction, the gap in black shale occurrence would indeed be similar in thickness to 405 kyr minima lower down in the Furlo section. What makes this interval remarkable, however, is that the number of black levels generally increases upsection, and that more black levels occur per bundle.

We discuss our observation on the interval below the Livello Bonarelli in more detail on page 14, lines 13–21, and include more information on other observations on the expression of 2.4 Myr eccentricity forcing in section 4.3.1 (p. 14-15).

Recent papers (Jenkyns et al. 2007; Gambacorta et al. 2015) reinterpreted the timing of Bonarelli Level at Furlo and Bottaccione relative to the phases of OAEII. Osmium-isotope excursion marking the onset of the event starts immediately beneath the Bonarelli Level at Furlo (du Vivier et al. 2014). Thus, the possibility that Bonarelli Level represents only the second buildup phase and plateau (page 7, lines 30-31) seems to be outdated (see, for example, figure 12 in Gambacorta et al. 2015). Does this change affect your estimate of the OAE II duration?

As our age model is not based on chemostratigraphic correlation, our estimate of OAE2 duration is not affected. The duration between the start of the $\delta^{13}C$ excursion and the C/T boundary is estimated at 490 kyr. We came to this value by taking into account the estimated duration of the Livello Bonarelli (based on time series analysis of high resolution XRF data), and the 405-kyr tuning for the interval between the top of the Livello Bonarelli and the C/T boundary. We do not consider a large hiatus as proposed by Gambacorta et al (2015) likely, as we have the first occurrence of *Quadrum gartneri* (see also next paragraph). A duration of 490 kyr between the onset of OAE2 and the C/T boundary is, within our stratigraphic uncertainty, in good agreement with the estimate of 538 kyr by Laurin et al. (2016), adapted from the work of Ma et al (2014) and Sageman et al (2006).

Gambacorta et al. (2015) interpret hiatuses in the upper part of the Bonarelli Level at Furlo and other sites in the Umbria-Marche Basin. Could you please indicate how are these hiatuses considered in your age model?

Hiatuses could occur at the sharp shifts in sedimentary facies at the base and the top of the Livello Bonarelli. If such hiatuses are (together) near 405 kyr in duration, they could result in a similar sedimentary rhythm and go unnoticed in our analyses. However, we would expect such a hiatus to have a more pronounced sedimentary expression. The potential for a hiatus at the base of the Livello Bonarelli was previously recognised by Jenkyns et al. (2007), and estimated to be on the order of 20 kyr. Such a hiatus would be small relatively to our tuning target, the 405 kyr periodicity of eccentricity. We would be happy to include a short paragraph on this issue in the revised version of the manuscript.

The discussion on the two points above is now included in the manuscript on page 12, lines 20-29.

Let me add a note on the paper by Lanci et al. (2010), which is criticized in your text. The phase calibration in this paper was based on a previous astronomical solution (La2004), and is probably incorrect as you noted. The change of interpretation is, however, not due to an incorrect sampling strategy by Lanci et al. (2010). We recently revisited the topic using the same data and simple numerical models. The results suggest that the omission of precession-paced organic layers in Lanci et al. (2010) does not distort the 100-kyr and 400-kyr eccentricity signatures to a degree that would prevent detection of 405-kyr eccentricity phases (Fig. S1.5 in the supporting information of Laurin et al., in press). I would not say that the sampling in Lanci et al. (2010) was “incorrect” (page 6, line 23 in your paper). It was correct considering that the authors needed to avoid lithological bias to focus on the record of changing bottom-water oxygenation in rock-magnetic properties. They just could not have assessed precession-scale variability, which is a major advantage of your color reflectance data.

We changed the wording of our criticism. However, in the revised version of the manuscript, we are still making clear that, if one does not take into account chert samples, the precession signal is largely eliminated in the intervals of the chert bundles while the weaker precession signal in the limestone beds

in between is kept. This is the reason why the precession filtered signal (Fig. 4b in Lanci et al., 2010) suggests the opposite (wrong) phase relation with eccentricity.

The wording on page 10, lines 9–14 is revised and includes a reference to the new interpretation of the data of Lanci et al. (2010) by Laurin et al (2016).

I believe the above issues can be fixed. Your paper includes important data and interpretations, and I am hoping to see the final version published soon.
Yours sincerely, Jiˇrí Laurin (Institute of Geophysics ASCR, Prague; laurin@ig.cas.cz)

Anonymous Referee #2

This study can be regarded as an extension of an earlier investigation on cyclicity and astrochronology of the same successions, published by Mitchell et al. 2008. This study includes a detailed C-isotope data set and it adds new radioisotope data. The results of this study are mostly in agreement with the earlier study. Additional information is gained on the mode of circulation during OAE2 and on the behaviour of the global carbon cycle before, during and after OAE2.

Carbon isotopes and carbon cycle:
Since the carbon isotope data are the most relevant new data in this study, the carbon isotope results deserve more in-depth discussion. The authors see an obliquity pattern in their data but they do not really discuss these data. In most Cretaceous data sets available from the literature, the obliquity pattern seems not preserved in C-isotope records, in few others there is some evidence, especially in the amplification of the signal within longer cycles (see Laurin et al.: .... "net transfers between reservoirs are plausibly controlled by ~1 Myr changes in the amplitude of axial obliquity"). The authors may add some comments on the obliquity – carbon residence time enigma in this study (see also Laurin et al. 2015).

The potential ~1 Myr cycle in the carbon isotope curve is very interesting and we are happy to include this in the discussion of long term orbital forcing and the carbon cycle in a revised version of the manuscript. In general, it seems that the trends in the carbon cycle follow a ~1 Myr pacing, whereas sharp excursions occur at ~2.4 Myr intervals superimposed on this pattern. The high resolution XRF data from the Livello Bonarelli show a likely obliquity pacing, as detected previously during OAE2 by Meyers et al. (2012). This observation likely reflects a long-term (~2.4 Myr) minimum in eccentricity-modulated precession, during which obliquity can become the dominant astronomical parameter driving changes in insolation, as was observed in the Eocene by Westerhold et al. (2014).

These observations are discussed in a new paragraph within section 4.3.1, on page 15, lines 8-24.

They may also discuss possible causes of the remarkable changes in the C-isotope pattern through time. The Turonian C- isotope curve is, across several long eccentricity cycles much more stable than the Cenomanian curve.
The authors may also comment on possible reasons, why the C- isotope pattern remains quite noisy throughout two eccentricity cycles from 476m to 484 m.

The Cenomanian carbon isotope curve indeed seems much more strongly paced by the 405 kyr cycle of eccentricity modulated precession than the Turonian $\delta^{13}C$ curve. A similar phenomenon was observed for the end of the Albian, and interpreted to reflect a change to a more stable ocean circulation pattern (Giorgioni et al., 2012). For the Cenomanian/Turonian, the carbon cycle may have become more stable as CO2 may have been drawn down by black shale formation and volcanic activity, delivering nutrients, may have decreased.

This view on the stability of the Turonian carbon isotope curve with respect to the Cenomanian curve is included on page 15, lines 25-29.

The high variability in $\delta^{13}C$ values from 476 to 484 m coincides with the frequent occurrence of organic-matter rich intervals. Potentially, this may have influenced the $\delta^{13}C$ values of, for example, early diagenetic cements.

This information is included on page 8 in lines 27–29.

Climate and oceanography:
It will be important to integrate new information on ocean chemistry, including new Nd- isotope data, into new ocean circulation models. It seems remarkable, that OAE 2 was characterised by a change in Tethys-Atlantic circulation, if Nd-isotope data are integrated into circulation reconstructions (e.g. Martin et al., 2012). An integration of geochemistry into improved circulation models will add value to this study which otherwise may be regarded just as a repetition of the Mitchell et al study. Carbon isotopes and
oceanography (p.6): Relatively low values of δ13C are be associated with stratification of the water column and reduced yearly integrated primary productivity (Sprovieri et al., 2013): » Do these peculiar

water mass conditions in the western Tethys control the C-isotope composition of the global marine carbon pool, or do you suggest “global stratification”? Conversely, high δ13C values likely do reflect good bottom water ventilation during eccentricity minima, with a prolonged avoidance of seasonal extremes, allowing for more stable primary productivity over the annual cycle which may have caused the increase in marine δ13C Â˜n see e.g. Nd-isotope work by e.g. Martin et al (2012) and others on deep-water formation during OAE 2.

We agree with the reviewer that new Nd-isotope data are essential for a better understanding of ocean circulation before and during OAE2. Although beyond the scope of this manuscript, this is part of the ongoing research by S. J. Batenburg. The Nd-isotope of Martin et al (2012) and others indicates a change in deep water formation and exchange at the Cenomanian-Turonian transition, which may have driven the transport of nutrients and black shale deposition. Such a change in circulation may have resulted from astronomically-forced changes in seasonality and the hydrological cycle.
As mentioned in the reply to reviewer #1, we highlight the differences between out manuscript and the Mitchell et al. (2008) study in the revised version of the manuscript. The remarks on the patterns in $\delta^{13}C$ values refer to the western Tethys, where regional anoxia already developed episodically before OAE2.

In the discussion, section 4.3.2 (pages 15-16) has been revised to incorporate more specific information on the potential effect of long-period astronomical forcing on hydrology and circulation. The differences with the Mitchell et al. (2008) study with regard to climatic mechanisms are discussed in more detail in this section, and the differences in tuning approach in section 4.2.2 (see also the reply to reviewer 1).

Figures
Please, add a stratigraphy figure to the chapter “geological setting” and to the regional map. This is fundamental information for the reader.

We gladly include a generalised stratigraphy of the Umbria-Marche basin next to the regional map in a revised version of the manuscript.

A generalised stratigraphy is now incorporated in Figure 1.

References

Eldrett, J. S., Ma, C., Bergman, S. C., Lutz, B., Gregory, F. J., Dodsworth, P., Phipps, M., Hardas, P., Minisini, D., Ozkan, A., Ramezani, J., Bowring, S. A., Kamo, S. L., Ferguson, K., Macaulay, C., and Kelly, A. E.: An astronomically calibrated stratigraphy of the Cenomanian, Turonian and earliest Coniacian from the Cretaceous Western Interior Seaway, USA: Implications for global chronostratigraphy, Cretaceous Research, 56, 316-344, 2015.

Gambacorta, G., Jenkyns, H. C., Russo, F., Tsikos, H., Wilson, P. A., Faucher, G., and Erba, E.: Carbon- and oxygen-isotope records of mid-Cretaceous Tethyan pelagic sequences from the Umbria – Marche and Belluno Basins (Italy), Newsletters on Stratigraphy, 48, 299-323, 10.1127/nos/2015/0066, 2015.

Giorgioni, M., Weissert, H., Bernasconi, S. M., Hochuli, P. A., Coccioni, R., and Keller, C. E.: Orbital control on carbon cycle and oceanography in the mid-Cretaceous greenhouse, Paleoceanography, 27, 10.1029/2011PA002163, 2012.

Jenkyns, H. C., Matthews, A., Tsikos, H., and Erel, Y.: Nitrate reduction, sulfate reduction, and sedimentary iron isotope evolution during the Cenomanian-Turonian oceanic anoxic event, Paleoceanography, 22, n/a-n/a, 10.1029/2006PA001355, 2007.

Kuiper, K. F., Deino, A., Hilgen, F. J., Krijgsman, W., Renne, P. R., and Wijbrans, J. R.: Synchronizing rock clocks of Earth history, Science, 320, 500-504, DOI 10.1126/science.1154339, 2008.

Lanci, L., Muttoni, G., and Erba, E.: Astronomical tuning of the Cenomanian Scaglia Bianca Formation at Furlo, Italy, Earth and Planetary Science Letters, 292, 231-237, 2010.

Laurin, J., Meyers, S. R., Galeotti, S., and Lanci, L.: Frequency modulation reveals the phasing of orbital eccentricity during Cretaceous Oceanic Anoxic Event II and the Eocene hyperthermals, Earth and Planetary Science Letters, 442, 143-156, 2016.

Ma, C., Meyers, S. R., Sageman, B. B., Singer, B. S., and Jicha, B. R.: Testing the astronomical time scale for oceanic anoxic event 2, and its extension into Cenomanian strata of the Western Interior Basin (USA), Geological Society of America Bulletin, 10.1130/b30922.1, 2014.

Martin, E. E., MacLeod, K. G., Jiménez Berrocoso, A., and Bourbon, E.: Water mass circulation on Demerara Rise during the Late Cretaceous based on Nd isotopes, Earth and Planetary Science Letters, 327–328, 111-120, 2012.

Meyers, S. R., Sageman, B. B., and Arthur, M. A.: Obliquity forcing of organic matter accumulation during Oceanic Anoxic Event 2, Paleoceanography, 27, 10.1029/2012pa002286, 2012.

Mitchell, R. N., Bice, D. M., Montanari, A., Cleaveland, L. C., Christianson, K. T., Coccioni, R., and Hinnov, L. A.: Oceanic anoxic cycles? Orbital prelude to the Bonarelli Level (OAE 2), Earth and Planetary Science Letters, 267, 1-16, 2008.

Renne, P. R., Swisher, C. C., Deino, A. L., Karner, D. B., Owens, T. L., and DePaolo, D. J.: Intercalibration of standards, absolute ages and uncertainties in 40Ar/39Ar dating, Chem Geol, 145, 117-152, 1998.

Sageman, B. B., Meyers, S. R., and Arthur, M. A.: Orbital time scale and new C-isotope record for Cenomanian-Turonian boundary stratotype, Geology, 34, 125-128, Doi 10.1130/G22074.1, 2006.

Westerhold, T., Röhl, U., Pälike, H., Wilkens, R., Wilson, P. A., and Acton, G.: Orbitally tuned timescale and astronomical forcing in the middle Eocene to early Oligocene, Clim. Past, 10, 955-973, 2014

List of relevant changes

(Page and line numbers refer to current manuscript)

P 3, l 3-25
Deleted: In the Umbria-Marche Basin (Fig. 1), the Livello Bonarelli separates the Cenomanian white limestones of the Scaglia Bianca from the Turonian pink limestones of the Scaglia Rossa. In this study, we present new geophysical and stable isotope data that were generated from the Cenomanian interval at the Furlo quarry, and from uppermost Cenomanian and Turonian deposits in the Gola del Bottaccione. In addition, stable carbon and oxygen isotope data were used from the Turonian of the Contessa quarry, published by Stoll and Schrag (2000). The proxy records from the Bottaccione, Contessa and Furlo sections are all presented on the same height scale, using the recent height scale for the Cretaceous Umbria-Marche basin introduced by Sprovieri et al. (2013).
Inserted:
Previous studies have investigated the rhythmic nature of the bedded limestones, (black) cherts and shales in sections near Gubbio (de Boer, 1982, 1983; Herbert and Fischer, 1986; Schwarzacher, 1994; Sprovieri et al., 2013) and at Furlo (Beaudouin et al., 1996; Mitchell et al., 2008; Lanci et al., 2010). In this study, we present new geophysical and stable isotope data generated from the Cenomanian interval at the Furlo quarry, and from uppermost Cenomanian and Turonian deposits in the Gola del Bottaccione (Fig. 1). In addition, stable carbon and oxygen isotope data from the Turonian of the Contessa quarry, published by Stoll and Schrag (2000) are used. The proxy records from the Bottaccione, Contessa and Furlo sections are all presented on the same height scale, using the recent height scale for the Cretaceous Umbria-Marche basin, introduced by Sprovieri et al. (2013).
In the Umbria-Marche Basin, the Livello Bonarelli separates the Cenomanian white limestones of the Scaglia Bianca from the Turonian pink limestones of the Scaglia Rossa. The strong changes in sedimentary facies necessitate the application of different proxy methods as archives for paleoclimatic variability. Colour reflectance was measured in the Cenomanian Scaglia Bianca, to capture the alternation of black cherts and shales with white limestones and light grey cherts. For the Turonian Scaglia Rossa, where colour variations are limited, magnetic susceptibility measurements reveal variations in the detrital contribution, as clastic particles are generally richer in ferromagnetic minerals. To investigate the Livello Bonarelli in high resolution, XRF data were generated, reflecting variations in detrital contribution (SiO_2, Al_2O_3, TiO_2) and organic matter content (Loss on ignition, LOI). High Al_2O_3 likely indicates a strong riverine input, in contrast to TiO_2, reflecting a stronger dust contribution. The SiO_2 can be both detrital and biogenic in origin. The LOI data reflect the weight of volatile substances lost upon heating and give a measure of the organic content.

P 4, l 3-4
Inserted:
Stable isotope ratios were measured on powders of all lithologies, and repeated with larger sample amounts when carbonate contents were insufficient.

P 6, l18-22
Deleted: 3 to 4 organic-rich levels, spaced ~20 cm apart (Figs. 2 & 3).
Inserted: 2 to 4 organic-rich levels, spaced ~20 cm apart (Figs. 2 & 3). Black cherts and shales increase in number up-section, although they are lacking in the interval between 483 and 485 m. Between 483.5 m and the Livello Bonarelli, the spacing between beds increases.

Despite this increase, the two thick cherts directly underlying the Livello Bonarelli display a similar grouping as the cherts throughout the section.

P 7, l 4
Deleted: circumflexes
Inserted: brackets

P 8, l 2
Deleted: circumflexes
Inserted: brackets

P 8, l 20 – P 9, l 22
Deleted: Stable isotopes and diagenesis
The records of $\delta^{18}O$ and $\delta^{13}C$ show long-term trends over the successions, although the $\delta^{18}O$ record in particular displays scatter which might be due to an influence of diagenesis. $\delta^{13}C$ is generally more robust to post-depositional alteration (Jenkyns et al., 1994) and bulk carbonate $\delta^{13}C$ patterns have been shown to be a powerful tool for stratigraphic correlation, despite variations in absolute values and amplitude amongst locations (Jarvis et al., 2006). Although variability at the sampling scale (3 cm) may partially represent effects of diagenesis which could obscure short (precessional scale) climatic signals, the longer term trends compare well with coeval sections in the Umbria-Marche basin (Stoll and Schrag, 2000; Sprovieri et al., 2013) and the English chalk records (Jarvis et al., 2006) (Figure 9).
Inserted: Proxy records and correlation of the C/T boundary
The records of $\delta^{18}O$ and $\delta^{13}C$ show long-term trends over the successions, although the $\delta^{18}O$ record in particular displays scatter, which might be due to an influence of diagenesis. The $\delta^{13}C$ signal is generally more robust to post-depositional alteration (Jenkyns et al., 1994) and bulk carbonate $\delta^{13}C$ patterns constitute a powerful tool for stratigraphic correlation, despite variations in absolute values and amplitude amongst locations (Jarvis et al., 2006). The Cenomanian record presented here displays a higher degree of variability than a recently published bulk carbonate $\delta^{13}C$ record from Furlo by Gambacorta et al. (2015). The high variability in $\delta^{13}C$ values from 476 to 484 m coincides with a frequent occurrence of organic-matter rich beds, which may have influenced $\delta^{13}C$ values of early diagenetic cements. Although variability at the sampling scale (3 cm) may partially represent effects of diagenesis which could obscure short (precessional scale) climatic signals, the longer term trends compare well with coeval sections in the Umbria-Marche basin (Sprovieri et al., 2013; Stoll and Schrag, 2000) and the English chalk records (Jarvis et al., 2006) (Fig. 9; see Section 4.5). Whereas the stable isotope data reflect variations in temperature, salinity and the global carbon cycle, with superimposed regional and diagenetic effects, the other proxy data are closely related to lithological variations. These lithological variations reflect differing contributions of detrital input (indicated by magnetic susceptibility, Al_2O_3, TiO_2, SiO_2) and biological productivity of organic matter, carbonate and biogenic silica (reflected in the colour reflectance, LOI and SiO_2 records). These variations show a local and direct response to orbitally-forced variations in temperature, run-off and ventilation.
In this study, the base of the Turonian stage at Bottaccione is placed at 487.47 m, just above the first occurrence of *Quadrum gartneri* at 487.25 m defining the base of the C11 zone (Sissingh, 1977), following Sprovieri et al. (2013) and Tsikos et al. (2004). Direct comparison of high resolution $\delta^{13}C_{carb}$ data from Pueblo (Caron et al., 2006) with $\delta^{13}C_{carb}$ data from Contessa (Stoll and Schrag, 2000) allows for correlating $\delta^{13}C_{carb}$ maximum III in Pueblo with the $\delta^{13}C_{carb}$ maximum 85 cm above the Livello Bonarelli at 487.52 cm, comparable with its location at Bottaccione. An alternative correlation places the C/T boundary near a

minimum in the $\delta^{13}C_{carb}$ data from the Gubbio S2 core (Trabucho-Alexandre et al., 2011) of Tsikos et al. (2004), which corresponds to the minimum in $\delta^{13}C_{carb}$ values at 488.22 m at Contessa (Stoll and Schrag, 2000), which is 75 cm above the C/T estimate adopted in this study.

P 9, l 23-24

Deleted: Astronomical forcing and phase relationships

Inserted: Astronomical forcing and calibration, 4.2.1Astronomical phase relations

P 10, l 9-14

Deleted: was deduced from the remanent magnetization within carbonates at Furlo (Lanci et al., 2010), incorrectly excluding cherts.

Inserted: is deduced from the remanent magnetization within carbonates at Furlo (Lanci et al., 2010), unfortunately excluding cherts and thereby obscuring the imprint of precession cycles on the sedimentary rhythms. By analysis of frequency modulation on the same dataset, Laurin et al. (2016) re-evaluated the phase relationship and concluded that periods of increased black chert deposition coincided with eccentricity maxima.

P11, l 3-25

Deleted: Anchoring the Astrochronology, Correlation of the C/T boundary

In this study, the base of the Turonian stage at Bottaccione is placed at 487.47 m, just above the first occurrence of *Quadrum gartneri* at 487.25 m defining the base of the C11 zone (Sissingh, 1977), following Sprovieri et al. (2013) and Tsikos et al. Direct comparison of high resolution $\delta^{13}C_{carb}$ data from Pueblo (Caron et al., 2006) with $\delta^{13}C_{carb}$ data from Contessa (Stoll and Schrag, 2001) allows for correlating $\delta^{13}C_{carb}$ maximum III in Pueblo with the $\delta^{13}C_{carb}$ maximum 85 cm above the Livello Bonarelli at 487.52 cm, comparable with its location at Bottaccione. An alternative correlation places the C/T boundary near a minimum in the $\delta^{13}C_{carb}$ data from the Gubbio S2 core (Trabucho-Alexandre et al., 2011) of Tsikos et al. (2004), which corresponds to the minimum in $\delta^{13}C_{carb}$ values at 488.22 m at Contessa (Stoll and Schrag, 2001), which is 75 cm above the C/T estimate adopted in this study. Consequently, 75 cm is taken as a conservative estimate of the stratigraphic uncertainty on the position of the C/T boundary, i.e. 487.47 ± 0.75 m. With an average sedimentation rate of 11 m/Myr, this stratigraphic error margin translates in a temporal uncertainty of ± 68 kyr.

Tuning options

Because of its stability, only the 405-kyr component of eccentricity can be used for astronomical tuning in the Cretaceous and not the ~100 kyr periodicity that was used in previous tuning efforts (Mitchell et al., 2008). The shorter obliquity and precession terms can only be used for the development of floating time scales.

Inserted: Calibration to 405-kyr eccentricity

In this study, we distinguish minima and maxima of the 405-kyr eccentricity cycle within the Scaglia Bianca and Scaglia Rossa by examining the band-pass filters of the geophysical proxies. Near the end of the dataset in Furlo, below the Livello Bonarelli, and for the Turonian interval above the Livello Bonarelli, the pattern of individual limestone-chert alternations is taken into account instead. The band-pass filters of the stable isotope data are presented to evaluate the cyclostratigraphic framework.

As mentioned above, multiple previous tuning efforts have been published on the Cenomanian-Turonian sections in the Umbria-Marche. However, the present study provides a clear advancement over previous reports because: (i) we use only the 405-kyr periodicity of eccentricity in the La2011 solution as tuning target; (ii) we present an independent estimate for the timespan from the base of the Livello Bonarelli to the C/T boundary; (iii) we use the calibrated age of 28.201 Ma (Kuiper et al., 2008) for the Fish canyon sanidine standard for

$^{40}Ar/^{39}Ar$ dating; and (iv) we provide a new radioisotopic age for the mid-Cenomanian event. We discuss each of these aspects in the following paragraphs.
We correlate interpreted 405-kyr eccentricity minima in the lithology and geophysical data to 405-kyr minima in the La2011 (nominal) eccentricity solution (Laskar et al., 2011a), obtained by band-pass filtering (300-625 kyr). Only the 405-kyr component of eccentric is stable beyond 50 Ma, and it is the prime tuning target for the Cretaceous. The shorter obliquity and eccentricity-modulated precession terms can only be used for the development of floating time scales. Previous tuning efforts have used the ~100 kyr periodicity of eccentricity (Mitchell et al., 2008), extracted from the La2004 solution, which is only considered reliable until 40 Ma (Laskar et al., 2004).

P 12, l 15-28
Deleted: , of 500-550 kyr and 450-500 kyr respectively, as well as in the Aristocrat-Angus-12-8 Core in Northern Colorado (Ma et al., 2014), of 516-613 kyr, albeit using a slightly different correlation
Inserted: (Meyers et al., 2012a), of 500-550 kyr and 450-500 kyr respectively, as well as in the Aristocrat-Angus-12-8 Core in Northern Colorado (Ma et al., 2014), of 516-613 kyr, and the Iona Core in Texas of ~540 kyr (Eldrett et al., 2015), albeit using slightly different correlations.
A potential complication arises from the sharp shifts in sedimentary facies at the base and the top of the Livello Bonarelli, which could be accompanied by hiatuses. A hiatus on the order of 20 kyr at the base of the black shale has been suggested by Jenkyns et al (2007). Such a hiatus would be relatively small compared to our tuning target, the 405-kyr periodicity of eccentricity-modulated precession. In contrast, Gambacorta et al. (2015) suggest a large hiatus near the top of the Livello Bonarelli, based on correlation of the phases of OAE2. This view is considered unlikely in this study, as there is no strong sedimentary expression of such a hiatus, the duration of black shale deposition estimated here is in good agreement with other studies and the first occurrence of *Quadrum gartneri* is detected 58 cm above the base of the Scaglia Rossa.

P12, l 32
Deleted: Although seemingly similar to a previously reported (Mitchell et al., 2008) tuned age of 94.21 Ma, the latter would correspond to an age of 94.81 Ma after recalibration to revised standard ages (Kuiper et al., 2008).

P13 l 1-9
Inserted: Integration with radioisotopic ages
The age for the base of the Livello Bonarelli of 94.19 ± 0.15 Ma (tuning #1) is similar to the previously reported age of 94.21 Ma (Mitchell et al., 2008). Nonetheless, Mitchell et al. (2008) used radioisotopic ages of Sageman et al. (2006), which were calculated using an age of 28.02 ± 0.28 Ma for the Fish Canyon sanidine standard (Renne et al., 1998), widely used in $^{40}Ar/^{39}Ar$ dating. In this study, ages are calculated with the recalibrated age of the Fish Canyon sanidine of 28.201 ± 0.046 Ma (σ) by Kuiper et al. (2008). Recalibration of the reported tuned age of 94.21 Ma (Mitchell et al., 2008) would correspond to an age of 94.81 Ma after recalibration to the revised standard age of Kuiper et al. (2008), a difference of 1.5 x 405-kyr cycle.

P 13, l 15
Deleted: Which can, however, not be excluded

P 13 l 18-28

Deleted: Although tuning #1 is in close agreement with the new $^{40}Ar/^{39}Ar$ age, both tuning options remain possible.

Inserted: Although tuning #2 is in better agreement with Eldrett et al. (2015), who reports an age for the onset of the OAE2 carbon isotope excursion of 94.64 ± 0.12 Ma, the correlation to radioisotopic ages leads us to favour the first tuning option. Tuning #1 is in close agreement with the new $^{40}Ar/^{39}Ar$ age for the mid-Cenomanian event, the intercalibrated age for Ash A at the base of the *Whiteinella archaeocretacea* zone and the age of the C/T boundary as determined by Meyers et al. (2012b).

P 14, l 2-16

Inserted: Expression of long-term eccentricity forcing

Superimposed on the hierarchical stacking patterns of lithologies in the studied succession, several features of the lithological and proxy records reveal the influence of long-term periodicities on local sedimentation and global climate. These observations include: (i) the absence of cherts in an interval below the Livello Bonarelli; (ii) a strong expression of obliquity forcing during deposition of the Livello Bonarelli, contemporaneous with a sedimentary response to the 100-kyr forcing of eccentricity; (iii) a spacing of 2.0 and 2.4 Myr, respectively, between the mid-Cenomanian $\delta^{13}C$ excursion, the onset of OAE2, and a positive $\delta^{13}C$ excursion in the mid-Turonian. These observations, in combination with a previously noted ~1 Myr cyclicity in $\delta^{13}C$, reveal a pacing of climatic events by long-term eccentricity cycles and will be further discussed in the following paragraphs.

Below the Livello Bonarelli, in the interval 483-485 m, black shales are conspicuously absent. This may partially be due to an increase in sedimentation rate, as indicated by a larger spacing between beds from 483.5 m upwards, but this pattern breaks the trend of an increasing number of black cherts and shales up-section, per meter as well as per interpreted ~100 kyr bundle. This may reflect the prolonged avoidance of seasonal extremes during long-term eccentricity minima of the 2.4-Myr cycle.

P 15, l 8 – P16, l 15

Deleted: The new astrochronologies allow for assessing the long-term behavior of the carbon cycle during the C/T transition. The onset of the MCE, the base of the Livello Bonarelli, and the middle of the negative $\delta^{13}C$ excursion of the mid-Turonian are separated by 2.0 Myr and 2.4 Myr, respectively. The 1.6 Myr long negative excursion in the mid-Turonian is characterized by an intermittent double positive peak ("Pewsey events"; Jarvis et al., 2006), similar to the MCE, starting at 91.7 Ma (tuning #1) or 92.1 Ma (tuning #2). These repetitive variations in $\delta^{13}C$, superimposed on the long-term behavior of the carbon cycle, are likely paced by the ~2.4-Myr eccentricity period. Following tuning #1, a tentative comparison with the full eccentricity solution La2011 (Fig. 2) reveals the occurrence of pronounced long-term minima in eccentricity before the mid-Cenomanian and mid-Turonian events.

Trace element studies indicate that volcanic activity of the Caribbean Large Igneous Province increasingly supplied nutrients and sulphate to a low-sulphate ocean, with a major pulse ~500 kyr before OAE2 (Snow et al., 2005; Jenkyns et al., 2007; Turgeon and Creaser, 2008; Adams et al., 2010). This is manifested by the increasing recurrence of black cherts through the Cenomanian interval, indicating that the western Tethys was progressively more prone to the development of anoxia due to a long-term trend of ongoing warming and increased volcanism. However, the exact timing of carbon cycle perturbations may be linked to a specific sequence of astronomical variations superimposed on this trend. The increased variability in seasonality, after the prolonged avoidance of seasonal extremes, was possibly

responsible for observed intensification of the hydrological cycle, weathering, and more vigorous ocean circulation.

Inserted: The new astrochronologies allow for assessing the long-term behaviour of the carbon cycle during the C/T transition. The onset of the MCE, the base of the Livello Bonarelli, and the middle of the negative $\delta^{13}C$ excursion of the mid-Turonian are separated by 2.0 Myr and 2.4 Myr, respectively. The 1.6 Myr long negative excursion in the mid-Turonian is characterized by an intermittent double positive peak ("Pewsey events"; Jarvis et al., 2006; Fig. 9), similar to the MCE, starting at 91.7 Ma (tuning #1) or 92.1 Ma (tuning #2). These repetitive variations in $\delta^{13}C$ are likely paced by the ~2.4-Myr eccentricity period. Following tuning #1, a tentative comparison with the full eccentricity solution La2011 (Fig. 2) reveals the occurrence of pronounced long-term minima in eccentricity before the mid-Cenomanian and mid-Turonian events. An influence of long-term (several Myr) cycles on $\delta^{13}C$ has been previously identified in a late Cretaceous $\delta^{13}C$ record from Bottaccione (Sprovieri et al., 2013). Recently, a ~1 Myr cycle was detected in the long term behaviour of $\delta^{13}C$, particularly in the Turonian record from the Bohemian Cretaceous Basin (Fig. 9), and attributed to the ~1.2 Myr cycle in amplitude modulation of Earth's axial obliquity (Laurin et al., 2015). Although a ~1 Myr periodicity cannot be identified in our data, an influence of obliquity forcing is observed in the Cenomanian part of the record. Sharp positive excursions on a ~2.4 Myr scale may have occurred superimposed on gradual ~1 Myr cycles in $\delta^{13}C$ variation.

The Cenomanian $\delta^{13}C$ curve is more strongly paced by the 405 kyr cycle than the Turonian $\delta^{13}C$ curve. Such a change was previously observed for the end of the Albian and interpreted to reflect a change to more stable ocean circulation patterns (Giorgioni et al., 2012). For the Cenomanian/Turonian, the carbon cycle may have become more stable as CO2 was drawn down by organic matter deposition and volcanic activity decreased.

Relation with volcanism

The increasing recurrence of black cherts through the Cenomanian interval indicates that the western Tethys was progressively more prone to the development of anoxia due to a long-term trend of on-going warming and increased volcanism. Trace element studies point to volcanic activity at the Caribbean Large Igneous Province as the supplier of nutrients and sulphate to a low-sulphate ocean, with a major pulse ~500 kyr before OAE2 (Snow et al., 2005; Turgeon and Creaser, 2008; Adams et al., 2010; Jenkyns et al., 2007). Volcanism is thus ultimately responsible for OAE2, but the exact timing of the onset of OAE2 seems to be linked to a specific sequence of astronomical variations superimposed on this trend. The increased variability in seasonality, after the prolonged avoidance of seasonal extremes, gave rise to an intensification of the hydrological cycle, weathering, and more vigorous ocean circulation, which is in agreement with several Nd-isotope records (Martin et al., 2012; Zheng et al., 2013) and Os isotope records (Du Vivier et al., 2014). Deep waters at Demerara Rise were replaced by bottom waters sourced from the Tethys and North Atlantic (Martin et al., 2012). Trabucho-Alexandre et al. (2010) suggest that the OAE2 interval may have been characterised by an intense estuarine circulation with upwelling in the proto-North Atlantic. This is consistent with the phase relationship inferred from our data: with black chert and shale deposition coincident with seasonality extremes during 405-kyr eccentricity maxima.

Other changes:

Figure 1 now includes a chrono- and lithostratigraphy of the Umbria-Marche succession in the Apennine mountains.

Figure 3 now has a clearer representation of the 100-kyr bundling, with brackets.

Orbital control on the timing of oceanic anoxia in the Late Cretaceous

S. J. Batenburg[1,2], D. De Vleeschouwer[3,4], M. Sprovieri[5], F. J. Hilgen[6], A. S. Gale[7], B. S. Singer[8], C. Koeberl[9,10], R. Coccioni[11], P. Claeys[4], A. Montanari[12]

[1] Department of Earth Sciences, University of Oxford, Oxford, United Kingdom

[2] Institut für Geowissenschaften, Goethe-Universität Frankfurt, Frankfurt am Main, Germany

[3] MARUM, Universität Bremen, Bremen, Germany

[4] Earth System Sciences, Vrije Universiteit Brussel, Brussels, Belgium

[5] IAMC-CNR Capo Granitola, Campobello di Mazara, Italy

[6] Department of Earth Sciences, Utrecht University, Utrecht, the Netherlands

[7] School of Earth and Environmental Sciences, University of Portsmouth, Portsmouth, United Kingdom

[8] Department of Geoscience, University of Wisconsin-Madison, Madison, Wisconsin, United States of America

[9] Department of Lithospheric Research, University of Vienna, Vienna, Austria

[10] Natural History Museum Vienna, Vienna, Austria

[11] Dipartimento di Scienze della Terra, della Vita e dell'Ambiente, Università degli Studi "Carlo Bo", Urbino, Italy

[12] Osservatorio Geologico di Coldigioco, 62020 Frontale di Apiro, Italy

Correspondence to: (sbatenburg@gmail.com)

Abstract

The oceans at the time of the Cenomanian-Turonian transition were abruptly perturbed by a period of bottom-water anoxia. This led to the brief but widespread deposition of black organic-rich shales, such as the Livello Bonarelli in the Umbria-Marche Basin (Italy). Despite

Deleted: disturbed

intensive studies, the origin and exact timing of this event are still debated. In this study, we assess leading hypotheses about the inception of oceanic anoxia in the Late Cretaceous greenhouse world, by providing a 6-Myr-long astronomically-tuned timescale across the Cenomanian-Turonian boundary. We procure insights in the relationship between orbital forcing and the Late Cretaceous carbon cycle by deciphering the imprint of astronomical cycles on lithologic, geophysical, and stable isotope records, obtained from the Bottaccione, Contessa and Furlo sections in the Umbria-Marche Basin. The deposition of black shales and cherts, as well as the onset of oceanic anoxia, is related to maxima in the 405-kyr cycle of eccentricity-modulated precession. Correlation to radioisotopic ages from the Western Interior (USA) provides unprecedented age control for the studied Italian successions. The most likely tuned age for the Livello Bonarelli base is 94.17 ± 0.15 Ma (tuning #1); however, a 405-kyr older age cannot be excluded (tuning #2) due to uncertainties in stratigraphic correlation, radioisotopic dating, and orbital configuration. Our cyclostratigraphic framework suggests that the exact timing of major carbon cycle perturbations during the Cretaceous may be linked to increased variability in seasonality (i.e. a 405-kyr eccentricity maximum) after the prolonged avoidance of seasonal extremes (i.e. a 2.4-Myr eccentricity minimum). Volcanism is probably the ultimate driver of oceanic anoxia, but orbital periodicities determine the exact timing of carbon cycle perturbations in the Late Cretaceous. This unites two leading hypotheses about the inception of oceanic anoxia in the Late Cretaceous greenhouse world.

Deleted: intense

Deleted: preferred tuning #1

Deleted: was

Deleted: was likely determined by orbital periodicities

1 Introduction

The organic rich Livello Bonarelli formed as a result of oxygen deficiency and carbonate dissolution in the oceans during the Cenomanian/Turonian (C/T) transition. During this Ocean Anoxic Event 2 (OAE2), a combination of factors caused increased productivity, incomplete decomposition of organic matter and widespread deposition of black shales. Although these sediments are intensively studied, the exact extent, cause, timing and duration of oceanic anoxia are debated (Sinton and Duncan, 1997; Mitchell et al., 2008). Contrasting causal mechanisms have been suggested, including stratification of the water column (Lanci et al., 2010) versus intensification of the hydrological cycle driving a dynamic ocean circulation (Trabucho-Alexandre et al., 2010). Studies on trace-elemental and (radiogenic) isotope compositions of Cenomanian marine successions have suggested a volcanic origin of OAE2, by delivering nutrients to the semi-enclosed proto-North Atlantic (Du Vivier et al., 2014;

Deleted: (Zheng et al., 2013, and references therein; Du Vivier et al., 2014).

Zheng et al., 2013; and references therein). Deciphering the importance of volcanic and oceanographic processes requires tight constraints on their relative timing. Regularly occurring black cherts and shales below the Livello Bonarelli demonstrate that oceanic conditions in the Umbria-Marche Basin were punctuated by episodes of regional anoxia from the mid-Cenomanian onwards. Their hierarchical stacking pattern suggests an orbital control on the deposition of organic rich horizons (Mitchell et al., 2008; Lanci et al., 2010). Stable carbon isotope data reveal that long-term variations in eccentricity paced the carbon cycle (Sprovieri et al., 2013) and sea level changes (Voigt et al., 2006) of the Late Cretaceous. Here we investigate the role of orbital forcing on climate and the carbon cycle, and, specifically, on organic-rich sedimentation prior, during, and after OAE2.

We also explore the potential for establishing an anchored astrochronology for the C/T interval in Europe. Recent improvements in the astronomical solution (La2011; Laskar et al., 2011b) and in the intercalibration of radiometric and astronomical dating techniques (Kuiper et al., 2008; Renne et al., 2013) allow the extension of the astronomical time scale into the Cretaceous. The C/T boundary in the Western Interior (USA) has been dated at 93.90 ± 0.15 Ma by intercalibration of radio-isotopic and astrochronologic time scales (Meyers et al., 2012b). Also, reinterpretation of proxy records spanning the C/T interval seems to resolve discrepancies in reported durations of the OAE2 (Meyers et al., 2012a; Sageman et al., 2006). The well-documented Italian rhythmic successions, reference sections for climatic processes in the Tethyan realm, need to be tied in with the numerical time scale. Biostratigraphic correlation to radioisotopically-dated ash beds in the Western Interior is complicated by the provinciality of faunas and floras. However, $\delta^{13}C$ stratigraphy provides a reliable correlation tool (Jenkyns et al., 1994) and we present a new $^{40}Ar/^{39}Ar$ age for the Thatcher bentonite from the Western Interior occurring within the mid-Cenomanian $\delta^{13}C$ event (MCE). This study integrates the well-developed cyclostratigraphy from the Umbria-Marche Basin with radioisotopic ages from the Western Interior and derives a numerical timescale for this critical interval in Earth's history.

Deleted: absolute

Deleted: (Gale et al., 2005)

2 Materials and Methods

2.1 Geological setting and proxy records

Previous studies have investigated the rhythmic nature of the bedded limestones, (black) cherts and shales in sections near Gubbio (de Boer, 1982, 1983; Herbert and Fischer, 1986; Schwarzacher, 1994; Sprovieri et al., 2013) and at Furlo (Beaudouin et al., 1996; Mitchell et al., 2008; Lanci et al., 2010). In this study, we present new geophysical and stable isotope data generated from the Cenomanian interval at the Furlo quarry, and from uppermost Cenomanian and Turonian deposits in the Gola del Bottaccione (Fig. 1). In addition, stable carbon and oxygen isotope data from the Turonian of the Contessa quarry, published by Stoll and Schrag (2000) are used. The proxy records from the Bottaccione, Contessa and Furlo sections are all presented on the same height scale, using the recent height scale for the Cretaceous Umbria-Marche basin, introduced by Sprovieri et al. (2013).

In the Umbria-Marche Basin, the Livello Bonarelli separates the Cenomanian white limestones of the Scaglia Bianca from the Turonian pink limestones of the Scaglia Rossa. The strong changes in sedimentary facies necessitate the application of different proxy methods as archives for paleoclimatic variability. Colour reflectance was measured in the Cenomanian Scaglia Bianca, to capture the alternation of black cherts and shales with white limestones and light grey cherts. For the Turonian Scaglia Rossa, where colour variations are limited, magnetic susceptibility measurements reveal variations in the detrital contribution, as clastic particles are generally richer in ferromagnetic minerals. To investigate the Livello Bonarelli in high resolution, XRF data were generated, reflecting variations in detrital contribution (SiO_2, Al_2O_3, TiO_2) and organic matter content (Loss on ignition, LOI). High Al_2O_3 likely indicates a strong riverine input, in contrast to TiO_2, reflecting a stronger dust contribution. The SiO_2 can be both detrital and biogenic in origin. The LOI data reflect the weight of volatile substances lost upon heating and give a measure of the organic content.

The W4 member of the Scaglia Bianca formation at Furlo (Coccioni, 1996) consists mainly of light grey to white pelagic biomicrite alternating with light grey nodular to bedded cherts and tabular black cherts (Mitchell et al., 2008). The section was logged in detail and sampled at 3 cm spacing with an electric handheld drill. The total light reflectance (L*, in %) was measured with a Konica Minolta Spectrophotometer CM 2002 on the surface of rock powders, recording the reflected energy (RSC) at 400 to 700 nm wavelengths in 10-nm steps (averaged

Deleted: In the Umbria-Marche Basin (Fig. 1), the Livello Bonarelli separates the Cenomanian white limestones of the Scaglia Bianca from the Turonian pink limestones of the Scaglia Rossa. In this study, we present new geophysical and stable isotope data that were generated from the Cenomanian interval at the Furlo quarry, and from uppermost Cenomanian and Turonian deposits in the Gola del Bottaccione. In addition, stable carbon and oxygen isotope data were used from the Turonian of the Contessa quarry, published by Stoll and Schrag (2000). The proxy records from the Bottaccione, Contessa and Furlo sections are all presented on the same height scale, using the recent height scale for the Cretaceous Umbria-Marche basin introduced by Sprovieri et al. (2013).

over three measurements). For the Furlo section, $\delta^{18}O$ and $\delta^{13}C$ were measured with a GasBench II device and a ThermoElectron Delta Plus XP mass spectrometer at the IAMC-CNR in Naples. Stable isotope ratios were measured on powders of all lithologies, and repeated with larger sample amounts when carbonate contents were insufficient.

The overlying Livello Bonarelli consists of alternating 5-50 mm layers of organic-rich black shale (up to 26% TOC) and lighter radiolarite (Kuroda et al., 2007). The Bonarelli interval was sampled at a 2 cm resolution at both the Furlo and Bottaccione sections. Contents of major and selected minor elements from the Livello Bonarelli were determined with a Philips PW2400 sequential X-ray fluorescence (XRF) spectrometer equipped with a Rh-excitation source at the University of Vienna. Details of the analytical procedures and accuracies are similar to those given in Reimold et al. (1994).

The overlying Turonian R1 member of the Scaglia Rossa formation consists of pink pelagic limestones and marly limestones with nodular to laminar red to gray cherts (Montanari et al., 1989). 38 m above the Livello Bonarelli at the Bottaccione section were logged in detail and the section was sampled at 5 cm spacing from 10 m to 30 m above the Livello Bonarelli. Magnetic Susceptibility (MS) was measured with a Bartington MS2B Dual Frequency magnetometer at the Osservatorio Geologico de Coldigioco (averaged over three measurements). Stable isotope ratios were measured with a Kiel III device coupled to a ThermoFinnigan delta+XL mass spectrometer at the Vrije Universiteit Brussel.

2.2 Ar/Ar dating

A new $^{40}Ar/^{39}Ar$ age was obtained for the mid-Cenomanian event in the $\delta^{13}C$ record. Sample 91-0-03 is the same material used by Obradovich (1993); it is from an ash bed in the *Conlinoceros gilberti* ammonite zone in the Western Interior (USA), commonly known as the Thatcher bentonite. Laser fusion $^{40}Ar/^{39}Ar$ analyses of single sanidine crystals were performed at the WiscAr laboratory, University of Wisconsin-Madison following methods detailed in Sageman et al. (2014). A total of 53 crystals were dated. Eleven crystals that yielded less than 98.5% radiogenic ^{40}Ar were excluded from the mean, as was one inherited crystal that gave an apparent age greater than 101 Ma. Ages are calculated relative to 28.201 ± 0.046 Ma Fish Canyon sanidines (Kuiper et al., 2008) using the ^{40}K decay constants of Min et al. (2000).

Deleted: From

Deleted: Loss on ignition data reflect the weight of volatile substances lost upon heating and give a measure of the organic content.

Deleted: 30m

Deleted: and

Deleted: Wiscoinisn

2.3 Time series analysis

Time series analysis was carried out using the MTM-method (Thomson, 1982) with LOWSPEC background estimation (Meyers, 2012), as implemented in the R package "astrochron" (Meyers, 2014). We used three 2-π prolate tapers and confidence levels were calculated with the LOWESS-based (Cleveland, 1979) procedure of Ruckstuhl et al. (2001). The Continuous Wavelet Transform is used to decompose the one-dimensional time-series into their two-dimensional time–frequency representation. Band-pass filters are applied with Analyseries (Paillard et al., 1996). Sedimentation rates within the Scaglia Rossa and Scaglia Bianca Formations are estimated with the Evolutionary Average Spectral Misfit (E-ASM) method (Meyers and Sageman, 2007), using all frequencies for which the MTM harmonic F-test reports a line component that exceeds 80% probability. For the Bonarelli level, sedimentation rate is estimated with the standard ASM method. Predicted orbital periods for the late Cretaceous (93 Ma) are from Berger et al. (1992).

3 Results

3.1 Lithology and proxy data

The Cenomanian black shales and cherts in the Furlo section display a hierarchical stacking pattern, with groups of 2 to 4 organic-rich levels, spaced ~20 cm apart (Figs. 2 & 3). Black cherts and shales increase in number up-section, although they are lacking in the interval between 483 and 485 m. Between 483.5 m and the Livello Bonarelli, the spacing between beds increases. Despite this increase, the two thick cherts directly underlying the Livello Bonarelli display a similar grouping as the cherts throughout the section. The total reflectance record (L*, in %) captures this stacking pattern: grey and black cherts reflect little light and display shifts towards lower L* values, in contrast to the bright micritic Scaglia Bianca limestones with high L* values. Increased variability and negative values of $\delta^{13}C$ and $\delta^{18}O$ coincide with higher variability in reflectance and with the occurrence of organic rich layers.

Deleted: 3 to 4 organic-rich levels, spaced ~20 cm apart (Figs. 2 & 3).

XRF data from the Livello Bonarelli at Furlo display a marked variability at a 12-cm scale (Fig. 4). The TiO_2, and Al_2O_3 records display very similar behaviour, whereas SiO_2, and LOI data additionally show variation on a 40-cm scale. At Bottaccione, a marked variability can be observed at an 8-cm scale in the SiO_2, TiO_2 and Al_2O_3 data from the Livello Bonarelli (Fig. 5).

The Scaglia Rossa pelagic limestones were studied in the classic Contessa and Bottaccione sections near Gubbio. Oscillations between radiolarian cherts and foram-coccolith pelagic limestones show hierarchical bundles of 2 to 5 chert layers per bundle. These bundles could be correlated amongst the Contessa and Bottaccione sections and are indicated by brackets on Figure 3. The lithologic log shown on Figure 3 is for the Bottaccione section. The magnetic susceptibility signal of the Bottaccione section accentuates the hierarchical stacking pattern, showing an increased magnetic susceptibility signal in intervals characterized by frequent chert beds (Fig. 3).

Deleted: circumflexes

Deleted: Figure

3.2 Ar/Ar

The inverse variance weighted mean age of 41 of the 53 sanidine crystals measured from sample 91-0-03 give an age of 96.21 ± 0.16/0.36 Ma (2σ analytical uncertainty/full uncertainty including decay constant and standard age), with an MSWD of 0.69 (Fig. 6). The complete set of analytical and standard data is in Suppl. Table 1.

Deleted: Figure

3.3 Time series analysis

Spectral analyses by MTM/LOWSPEC, in combination with the evolutionary Average Spectral Misfit (ASM; Meyers and Sageman, 2007) method, suggest an average sedimentation rate around 11 m/Myr throughout the studied interval, excluding the Livello Bonarelli (Figs. 7 & 8).

In the Cenomanian interval, the MTM/LOWSPEC spectra of all proxies exhibit a spectral peak exceeding the 95% CL for a cycle thickness of 0.25 m, corresponding to the spacing between individual chert layers, which is interpreted as the imprint of ~21-kyr precession (left column in Fig. 7). The average accumulation rate is 11 m/Myr (lower panel in Fig. 8) and the dominant periodicities at 1 and 4 m correspond to 100-kyr and 405-kyr eccentricity, respectively (Fig. 7).

Similarly, in the Turonian interval, a 0.25 m spectral peak exceeds the 95% CL for all proxies and is interpreted as the imprint of precession (right column in Fig. 7). Here, the eccentricity components are represented by dominant periodicities of 4.66 and 1.16 m and the average accumulation rate is 10.5 m/Myr (upper panel in Fig. 8).

We also find a statistically significant imprint of obliquity in Furlo's Cenomanian $\delta^{13}C$ record which confirms an important obliquity-control on the greenhouse carbon cycle, as suggested

by Laurin et al. (2015). Grouping of precession-related chert-limestone alternations in ~100-kyr bundles is indicated by brackets next to the lithological log in Fig. 3 and 405-kyr eccentricity cycles are denoted by yellow-white alternating bands. The definition of eccentricity minima and maxima is based on the extremes of the 3-5 m bandpass filter of L* (Furlo), MS (Bottaccione), as well as and on the stacking pattern of shales and cherts (Bottaccione).

For the Livello Bonarelli from Furlo (124 cm), a duration estimate is obtained from 2-cm spaced X-Ray Fluorescence (XRF) spectrometry data. The multitaper method (MTM) spectral analyses of SiO_2 yield dominant periodicities of ~40, ~12, and ~6 cm (Fig. 3a). We calculate the ASM using the results of MTM harmonic analysis (>80%), and obtain an optimal sedimentation rate of 0.286 cm/kyr for the Bonarelli in Furlo. Hence, we interpret the reported periodicities as the imprint of short eccentricity, obliquity, and precession and estimate the duration of the Livello Bonarelli at 413 kyr.

ASM analysis of the Al_2O_3 data from the 82 cm thick Livello Bonarelli at Bottaccione suggests an optimal sedimentation rate of 0.208 cm/kyr (Fig. 5). The ~8-cm thick cycles are interpreted as the imprint of obliquity and the duration of Livello Bonarelli at Bottaccione is estimated at 410 kyr, comparable to the estimate of 413 kyr at Furlo.

Deleted: circumflexes

Deleted: ,

Deleted: yr

4 Discussion

4.1 Proxy records and correlation of the C/T boundary

The records of $\delta^{18}O$ and $\delta^{13}C$ show long-term trends over the successions, although the $\delta^{18}O$ record in particular displays scatter, which might be due to an influence of diagenesis. The $\delta^{13}C$ signal is generally more robust to post-depositional alteration (Jenkyns et al., 1994) and bulk carbonate $\delta^{13}C$ patterns constitute a powerful tool for stratigraphic correlation, despite variations in absolute values and amplitude amongst locations (Jarvis et al., 2006). The Cenomanian record presented here displays a higher degree of variability than a recently published bulk carbonate $\delta^{13}C$ record from Furlo by Gambacorta et al. (2015). The high variability in $\delta^{13}C$ values from 476 to 484 m coincides with a frequent occurrence of organic-matter rich beds, which may have influenced $\delta^{13}C$ values of early diagenetic cements. Although variability at the sampling scale (3 cm) may partially represent effects of diagenesis which could obscure short (precessional scale) climatic signals, the longer term trends

compare well with coeval sections in the Umbria-Marche basin (Sprovieri et al., 2013; Stoll and Schrag, 2000) and the English chalk records (Jarvis et al., 2006) (Fig. 9; see Section 4.5).

Whereas the stable isotope data reflect variations in temperature, salinity and the global carbon cycle, with superimposed regional and diagenetic effects, the other proxy data are closely related to lithological variations. These lithological variations reflect differing contributions of detrital input (indicated by magnetic susceptibility, Al_2O_3, TiO_2, SiO_2) and biological productivity of organic matter, carbonate and biogenic silica (reflected in the colour reflectance, LOI and SiO_2 records). These variations show a local and direct response to orbitally-forced variations in temperature, run-off and ventilation.

In this study, the base of the Turonian stage at Bottaccione is placed at 487.47 m, just above the first occurrence of *Quadrum gartneri* at 487.25 m defining the base of the C11 zone (Sissingh, 1977), following Sprovieri et al. (2013) and Tsikos et al. (2004). Direct comparison of high resolution $\delta^{13}C_{carb}$ data from Pueblo (Caron et al., 2006) with $\delta^{13}C_{carb}$ data from Contessa (Stoll and Schrag, 2000) allows for correlating $\delta^{13}C_{carb}$ maximum III in Pueblo with the $\delta^{13}C_{carb}$ maximum 85 cm above the Livello Bonarelli at 487.52 cm, comparable with its location at Bottaccione. An alternative correlation places the C/T boundary near a minimum in the $\delta^{13}C_{carb}$ data from the Gubbio S2 core (Trabucho-Alexandre et al., 2011) of Tsikos et al. (2004), which corresponds to the minimum in $\delta^{13}C_{carb}$ values at 488.22 m at Contessa (Stoll and Schrag, 2000), which is 75 cm above the C/T estimate adopted in this study. Consequently, 75 cm is taken as a conservative estimate of the stratigraphic uncertainty on the position of the C/T boundary, i.e. 487.47 ± 0.75 m. With an average sedimentation rate of 11 m/Myr, this stratigraphic error margin translates in a temporal uncertainty of ± 68 kyr.

Moved (insertion) [1]

4.2 Astronomical forcing and calibration

Deleted: <#>Stable isotopes and diagenesis ... [1]

4.2.1 Astronomical phase relations

Deleted: relationships

Throughout the Cenomanian interval of the Furlo section, black cherts occur in distinct bands, which are often underlain by a thin layer of black shale. As these organic-rich horizons do not occur as nodules, they reflect a primary silica enrichment from radiolarian and/or diatom blooms. When present, black chert bands occur in groups with a regular spacing amongst them, likely reflecting a threshold response to extremes of the precessional cycle. Previous tuning attempts have placed black cherts either in eccentricity maxima (Mitchell et al., 2008; Voigt et al., 2006) or eccentricity minima (Lanci et al., 2010), entailing distinctly different

oceanographic regimes. During eccentricity maxima, the seasonal contrast on the Northern Hemisphere is periodically enhanced during high-amplitude precession minima, thereby intensifying monsoons, leading to an estuarine circulation in the Cretaceous North Atlantic with upwelling and increased productivity (Mitchell et al., 2008), potentially spurred by input of nutrients from volcanic activity (Trabucho-Alexandre et al., 2010). Alternatively, it has been suggested that eccentricity minima could cause decreased seasonality, leading to stagnation and reduced ventilation of bottom waters (Lanci et al., 2010; Herbert and Fischer, 1986), although eccentricity minima would not lower seasonality but rather avoid large seasonal extremes for a prolonged period of time. This reverse phase relationship is deduced from the remanent magnetization within carbonates at Furlo (Lanci et al., 2010), unfortunately excluding cherts and thereby obscuring the imprint of precession cycles on the sedimentary rhythms. By analysis of frequency modulation on the same dataset, Laurin et al. (2016) re-evaluated the phase relationship and concluded that periods of increased black chert deposition coincided with eccentricity maxima.

The relationship between eccentricity forcing and ocean-climate response can be derived from the degree of variability in the presented data. Intervals marked by maximal lithological difference represent periods of large precessional amplitude during eccentricity maxima. Radiolarian cherts coincide with maximal amplitude of carbon and oxygen isotope signals and with a tendency of those proxies towards more negative values (Figs. 2 & 3). Negative $\delta^{18}O$ values may reflect warmer temperatures and a potentially increased influx of fresh water by increased monsoonal activity. Relatively low values of $\delta^{13}C$ could be associated with stratification of the water column and reduced yearly integrated primary productivity (Sprovieri et al., 2013). Conversely, high $\delta^{13}C$ values likely reflect good bottom water ventilation during eccentricity minima, with a prolonged avoidance of seasonal extremes, allowing for more stable primary productivity over the annual cycle that may have caused the increase in marine $\delta^{13}C$ (Fig. 3). Possibly, the increased accumulation of organic carbon on land due to more uniform annual precipitation during eccentricity minima may have amplified the rise in marine $\delta^{13}C$, as suggested for Cenozoic intervals (Zachos et al., 2010). Figure 2 illustrates this phase relationship based on proxy records from the Cenomanian Furlo section. An analogous phase relationship for the proxy records from the Bottaccione sections is inferred. There, black cherts are absent from the Turonian interval of the succession, but grey cherts occur rhythmically throughout. Increased variability and negative values of $\delta^{13}C$

Deleted: (Lanci et al., 2010)

Deleted: was deduced from the remanent magnetization within carbonates at Furlo (Lanci et al., 2010), incorrectly excluding cherts.

Deleted: Figures

Deleted: integrated primary productivity (Sprovieri et al., 2013).

Deleted: which

Deleted: Figure

Deleted: was

coincide with high variability in the magnetic susceptibility record in chert-rich intervals, associated with eccentricity maxima.

4.2.2 Calibration to 405-kyr eccentricity

In this study, we distinguish minima and maxima of the 405-kyr eccentricity cycle within the Scaglia Bianca and Scaglia Rossa by examining the band-pass filters of the geophysical proxies. Near the end of the dataset in Furlo, below the Livello Bonarelli, and for the Turonian interval above the Livello Bonarelli, the pattern of individual limestone-chert alternations is taken into account instead. The band-pass filters of the stable isotope data are presented to evaluate the cyclostratigraphic framework.

As mentioned above, multiple previous tuning efforts have been published on the Cenomanian-Turonian sections in the Umbria-Marche. However, the present study provides a clear advancement over previous reports because: (i) we use only the 405-kyr periodicity of eccentricity in the La2011 solution as tuning target; (ii) we present an independent estimate for the timespan from the base of the Livello Bonarelli to the C/T boundary; (iii) we use the calibrated age of 28.201 Ma (Kuiper et al., 2008) for the Fish canyon sanidine standard for $^{40}Ar/^{39}Ar$ dating; and (iv) we provide a new radioisotopic age for the mid-Cenomanian event. We discuss each of these aspects in the following paragraphs.

We correlate interpreted 405-kyr eccentricity minima in the lithology and geophysical data to 405-kyr minima in the La2011 (nominal) eccentricity solution (Laskar et al., 2011a), obtained by band-pass filtering (300-625 kyr). Only the 405-kyr component of eccentric is stable beyond 50 Ma, and it is the prime tuning target for the Cretaceous. The shorter obliquity and eccentricity-modulated precession terms can only be used for the development of floating time scales. Previous tuning efforts have used the ~100 kyr periodicity of eccentricity (Mitchell et al., 2008), extracted from the La2004 solution, which is only considered reliable until 40 Ma (Laskar et al., 2004).

Two 405-kyr tuning options to astronomical solution La2011 remain if a C/T boundary age of 93.9 ± 0.15 Ma (Sageman et al., 2006; Meyers et al., 2012b) is considered, along with stratigraphic uncertainty in the studied sections (± 0.068 Ma) and uncertainty in the astronomical solution. The uncertainty in the 405-kyr component of the astronomical target curve was estimated at ± 78.5 kyr, by determining the maximal difference between the

Deleted: . ... [2]

Deleted: . Direct comparison of high resolution $\delta^{13}C_{carb}$ data from Pueblo (Caron et al., 2006) with $\delta^{13}C_{carb}$ data from Contessa (Stoll and Schrag, 2001) allows for correlating $\delta^{13}C_{carb}$ maximum III in Pueblo with the $\delta^{13}C_{carb}$ maximum 85 cm above the Livello Bonarelli at 487.52 cm, comparable with its location at Bottaccione. An alternative correlation places the C/T boundary near a minimum in the $\delta^{13}C_{carb}$ data from the Gubbio S2 core (Trabucho-Alexandre et al., 2011) of Tsikos et al. (2004), which corresponds to the minimum in $\delta^{13}C_{carb}$ values at 488.22 m at Contessa (Stoll and Schrag, 2001), which is 75 cm above the C/T estimate adopted in this study.

Moved up [1]: Consequently, 75 cm is taken as a conservative estimate of the stratigraphic uncertainty on the position of the C/T boundary, i.e. 487.47 ± 0.75 m. With an average sedimentation rate of 11 m/Myr, this stratigraphic error margin translates in a temporal uncertainty of ± 68 kyr.

Deleted: . ... [3]

Deleted: uncertainty

position of minima in the 405-kyr band-pass filter outputs (300-625 kyr) of the La2010d, La2011 and La2011m2 solutions (Laskar et al., 2011a). The first 405-kyr minimum in the Turonian at 489.1 m in Bottaccione corresponds to the 405-kyr minimum in the astronomical solution at 93.5 ± 0.15 (tuning #1) or at 93.9 ± 0.15 Ma (tuning #2; Fig. 3).

Tuning options for the Cenomanian interval of this study depend on the duration of the Livello Bonarelli. The Livello Bonarelli in the Umbria-Marche basin reflects the culmination of OAE2, limited to the "2nd-build-up" and "plateau" of the OAE2 $\delta^{13}C$ excursion (Tsikos et al., 2004). The estimated duration in this study between the start of the $\delta^{13}C$ excursion, below the Livello Bonarelli, and the Cenomanian-Turonian boundary is ~490 kyr. This duration is slightly longer than a previous estimate from the German Wunstorf core of 430-445 kyr for the OAE2 isotope excursion (Takashima et al., 2009; Voigt et al., 2008), and slightly shorter than the duration of of 520 – 560 kyr from the "first build-up" to the "end of plateau", determined by intercalibration between radioisotopic and astrochronologic time-scales at the C/T GSSP (Sageman et al., 2006; Meyers et al., 2012b). Similar duration estimates for this interval were obtained by reinterpreting the orbital influence at Demerara Rise and Tarfaya (Meyers et al., 2012a), of 500-550 kyr and 450-500 kyr respectively, as well as in the Aristocrat-Angus-12-8 Core in Northern Colorado (Ma et al., 2014), of 516-613 kyr, and the Iona Core in Texas of ~540 kyr (Eldrett et al., 2015), albeit using slightly different correlations.

Deleted: , of 500-550 kyr and 450-500 kyr respectively, as well as in the Aristocrat-Angus-12-8 Core in Northern Colorado (Ma et al., 2014), of 516-613 kyr, albeit using a slightly different correlation

A potential complication arises from the sharp shifts in sedimentary facies at the base and the top of the Livello Bonarelli, which could be accompanied by hiatuses. A hiatus on the order of 20 kyr at the base of the black shale has been suggested by Jenkyns et al (2007). Such a hiatus would be relatively small compared to our tuning target, the 405-kyr periodicity of eccentricity-modulated precession. In contrast, Gambacorta et al. (2015) suggest a large hiatus near the top of the Livello Bonarelli, based on correlation of the phases of OAE2. This view is considered unlikely in this study, as there is no strong sedimentary expression of such a hiatus, the duration of black shale deposition estimated here is in good agreement with other studies and the first occurrence of *Quadrum gartneri* is detected 58 cm above the base of the Scaglia Rossa.

The duration estimate for the Livello Bonarelli allows the extension of the astronomical tuning into the Cenomanian interval of this study. The base of the Livello Bonarelli corresponds to

94.19 ± 0.15 Ma (tuning #1) or 94.59 ± 0.15 Ma (tuning #2); i.e., the first short-eccentricity maximum after a 405-kyr minimum.

4.2.3 Integration with radioisotopic ages

The age for the base of the Livello Bonarelli of 94.19 ± 0.15 Ma (tuning #1) is similar to the previously reported age of 94.21 Ma (Mitchell et al., 2008). Nonetheless, Mitchell et al. (2008) used radioisotopic ages of Sageman et al. (2006), which were calculated using an age of 28.02 ± 0.28 Ma for the Fish Canyon sanidine standard (Renne et al., 1998), widely used in $^{40}Ar/^{39}Ar$ dating. In this study, ages are calculated with the recalibrated age of the Fish Canyon sanidine of 28.201 ± 0.046 Ma (σ) by Kuiper et al. (2008). Recalibration of the reported tuned age of 94.21 Ma (Mitchell et al., 2008) would correspond to an age of 94.81 Ma after recalibration to the revised standard age of Kuiper et al. (2008), a difference of 1.5 x 405-kyr cycle.

Additional age control is provided by correlation of two Cenomanian ash beds from the Western Interior of the USA. Correlation to "Ash A" at the base of the boundary of the planktonic foraminifer biozones of *Whiteinella archaeocretacea* and *Rotalipora cushmani* (Sageman et al., 2006; Caron et al., 2006; Leckie, 1985) provides an independent age for this zonal boundary 7 cm below the base of the Bonarelli Level of 94.20 ± 0.28 Ma. This age is in closer agreement to tuning #1 (94.17 ± 0.15 Ma) than to tuning #2 (94.57 ± 0.15 Ma).

The MCE, characterized by a double positive peak in $\delta^{13}C$ at Furlo (first maximum at 466.47 m), offers another opportunity to test both tuning options. The $^{40}Ar/^{39}Ar$ isotope data were acquired from 41 single sanidine crystals in sample 91-O-03 of Obradovich (1993) (methods outlined in Sageman et al., 2014), and yields an age of 96.21 ± 0.16/0.36 (2σ analytical and full uncertainty) for the Thatcher bentonite in the *Conlinceras tarrantense* zone at Pueblo, Colorado. This bentonite falls within the first peak of the MCE (Gale et al., 2008). In our tuning options, this level is either 96.09 ± 0.15 Ma (tuning #1) or 96.49 ± 0.15 Ma (tuning #2). Although tuning #2 is in better agreement with Eldrett et al. (2015), who reports an age for the onset of the OAE2 carbon isotope excursion of 94.64 ± 0.12 Ma, the correlation to radioisotopic ages leads us to favour the first tuning option. Tuning #1 is in close agreement with the new $^{40}Ar/^{39}Ar$ age for the mid-Cenomanian event, the intercalibrated age for Ash A at the base of the *Whiteinella archaeocretacea* zone and the age of the C/T boundary as determined by Meyers et al. (2012b). Nonetheless, the duration between radioisotopic age tie-points is consistent with cyclostratigraphy (Fig. 2) and provides tuned ages for biostratigraphic events (Table 1).

Deleted: Although seemingly similar to a previously reported (Mitchell et al., 2008) tuned age of 94.21 Ma, the latter would correspond to an age of 94.81 Ma after recalibration to revised standard ages (Kuiper et al., 2008).

Deleted: ... [4]

Deleted:), which can, however, not be excluded.

Deleted: . In our tuning options, this level is either 96.09 ± 0.15 Ma (tuning #1) or 96.49 ± 0.15 Ma (tuning #2). Although tuning #1 is in close agreement with the new $^{40}Ar/^{39}Ar$ age, both tuning options remain possible.

4.3 Long term behaviour of the carbon cycle

4.3.1 Expression of long-term eccentricity forcing

Superimposed on the hierarchical stacking patterns of lithologies in the studied succession, several features of the lithological and proxy records reveal the influence of long-term periodicities on local sedimentation and global climate. These observations include: (i) the absence of cherts in an interval below the Livello Bonarelli; (ii) a strong expression of obliquity forcing during deposition of the Livello Bonarelli, contemporaneous with a sedimentary response to the 100-kyr forcing of eccentricity; (iii) a spacing of 2.0 and 2.4 Myr, respectively, between the mid-Cenomanian $\delta^{13}C$ excursion, the onset of OAE2, and a positive $\delta^{13}C$ excursion in the mid-Turonian. These observations, in combination with a previously noted ~1 Myr cyclicity in $\delta^{13}C$, reveal a pacing of climatic events by long-term eccentricity cycles and will be further discussed in the following paragraphs.

Below the Livello Bonarelli, in the interval 483-485 m, black shales are conspicuously absent. This may partially be due to an increase in sedimentation rate, as indicated by a larger spacing between beds from 483.5 m upwards, but this pattern breaks the trend of an increasing number of black cherts and shales up-section, per meter as well as per interpreted ~100 kyr bundle. This may reflect the prolonged avoidance of seasonal extremes during long-term eccentricity minima of the 2.4-Myr cycle. The first ~100-kyr bundle of black cherts following this interval contains exceptionally thick dark levels and corresponds to the beginning of the first 405-kyr maximum after the ~2.4-Myr minimum. Hence, we associate the onset of OAE2 with this 405-kyr maximum.

Within the Livello Bonarelli, the imprint of 100-kyr eccentricity cycles can be observed, comparable to the expression of OAE2 in the Sicilian Calabianca section (Scopelliti et al., 2006) and in the German Wunstorf core (Voigt et al., 2008). Additionally, ten obliquity-related cycles can be visually detected in the XRF-proxy data (Fig. 4b-e). Silica, delivered by radiolarian blooms, mirrors terrestrially derived components (Al_2O_3 and TiO_2) and may represent variations in seasonality and ventilation driven by obliquity during the deposition of the Livello Bonarelli.

Two pronounced 405 kyr minima, likely within a 2.4 Myr minimum, occur in the upper Cenomanian, the first of which could correspond (following tuning #1) to the interval lacking black shales at 483-485 m, and the second occurring within the Livello Bonarelli. The

Deleted: Although

Deleted: occurrence of black layers increases up-section at Furlo, black cherts and shales are absent

Deleted: one can also visually observe

Deleted: (Voigt et al., 2008). Ten obliquity

occurrence of two 405 kyr minima within a 2.4 Myr minimum could explain the observed presence of the ~100 kyr cyclicity within the Livello Bonarelli, as well as the influence of obliquity, also detected during OAE2 in several North Atlantic datasets (Meyers et al., 2012a). The Livello Bonarelli was previously suggested to coincide with a 2.4 Myr eccentricity minimum, invoking stagnation as forcing mechanism for anoxia (Mitchell et al., 2008). The relatively strong obliquity influence during the deposition of the Livello Bonarelli is consistent with this orbital configuration (Hilgen et al., 2003).

The new astrochronologies allow for assessing the long-term behaviour of the carbon cycle during the C/T transition. The onset of the MCE, the base of the Livello Bonarelli, and the middle of the negative $\delta^{13}C$ excursion of the mid-Turonian are separated by 2.0 Myr and 2.4 Myr, respectively. The 1.6 Myr long negative excursion in the mid-Turonian is characterized by an intermittent double positive peak ("Pewsey events"; Jarvis et al., 2006; Fig. 9), similar to the MCE, starting at 91.7 Ma (tuning #1) or 92.1 Ma (tuning #2). These repetitive variations in $\delta^{13}C$ are likely paced by the ~2.4-Myr eccentricity period. Following tuning #1, a tentative comparison with the full eccentricity solution La2011 (Fig. 2) reveals the occurrence of pronounced long-term minima in eccentricity before the mid-Cenomanian and mid-Turonian events. An influence of long-term (several Myr) cycles on $\delta^{13}C$ has been previously identified in a late Cretaceous $\delta^{13}C$ record from Bottaccione (Sprovieri et al., 2013). Recently, a ~1 Myr cycle was detected in the long term behaviour of $\delta^{13}C$, particularly in the Turonian record from the Bohemian Cretaceous Basin (Fig. 9), and attributed to the ~1.2 Myr cycle in amplitude modulation of Earth's axial obliquity (Laurin et al., 2015). Although a ~1 Myr periodicity cannot be identified in our data, an influence of obliquity forcing is observed in the Cenomanian part of the record. Sharp positive excursions on a ~2.4 Myr scale may have occurred superimposed on gradual ~1 Myr cycles in $\delta^{13}C$ variation.

The Cenomanian $\delta^{13}C$ curve is more strongly paced by the 405 kyr cycle than the Turonian $\delta^{13}C$ curve. Such a change was previously observed for the end of the Albian and interpreted to reflect a change to more stable ocean circulation patterns (Giorgioni et al., 2012). For the Cenomanian/Turonian, the carbon cycle may have become more stable as CO2 was drawn down by organic matter deposition and volcanic activity decreased.

4.3.2 Relation with volcanism

The increasing recurrence of black cherts through the Cenomanian interval indicates that the western Tethys was progressively more prone to the development of anoxia due to a long-

Deleted: which was

Deleted: might be

Deleted: The new astrochronologies allow for assessing the long-term behavior of the carbon cycle during the C/T transition. The onset of the MCE, the base of the Livello Bonarelli, and the middle of the negative $\delta^{13}C$ excursion of the mid-Turonian are separated by 2.0 Myr and 2.4 Myr, respectively. The 1.6 Myr long negative excursion in the mid-Turonian is characterized by an intermittent double positive peak ("Pewsey events"; Jarvis et al., 2006), similar to the MCE, starting at 91.7 Ma (tuning #1) or 92.1 Ma (tuning #2). These repetitive variations in $\delta^{13}C$, superimposed on the long-term behavior of the carbon cycle, are likely paced by the ~2.4-Myr eccentricity period. Following tuning #1, a tentative comparison with the full eccentricity solution La2011 (Fig. 2) reveals the occurrence of pronounced long-term minima in eccentricity before the mid-Cenomanian and mid-Turonian events. ... [5]

Deleted: , indicating

term trend of on-going warming and increased volcanism. Trace element studies point to volcanic activity at the Caribbean Large Igneous Province as the supplier of nutrients and sulphate to a low-sulphate ocean, with a major pulse ~500 kyr before OAE2 (Snow et al., 2005; Turgeon and Creaser, 2008; Adams et al., 2010; Jenkyns et al., 2007). Volcanism is thus ultimately responsible for OAE2, but the exact timing of the onset of OAE2 seems to be linked to a specific sequence of astronomical variations superimposed on this trend. The increased variability in seasonality, after the prolonged avoidance of seasonal extremes, gave rise to an intensification of the hydrological cycle, weathering, and more vigorous ocean circulation, which is in agreement with several Nd-isotope records (Martin et al., 2012; Zheng et al., 2013) and Os isotope records (Du Vivier et al., 2014). Deep waters at Demerara Rise were replaced by bottom waters sourced from the Tethys and North Atlantic (Martin et al., 2012). Trabucho-Alexandre et al. (2010) suggest that the OAE2 interval may have been characterised by an intense estuarine circulation with upwelling in the proto-North Atlantic. This is consistent with the phase relationship inferred from our data: with black chert and shale deposition coincident with seasonality extremes during 405-kyr eccentricity maxima. Previously, Mitchell et al. (2008) placed OAE2 within the ~2.4 Myr minimum itself and suggested that the lack of strong insolation variability, associated with such a minimum, prevented the system from changing states and hindered limestone deposition. However, our chronology advocates intensified circulation and upwelling, delivering nutrients from volcanism and weathering to the western Tethys and the North Atlantic, and triggering prolonged and widespread anoxia. In conclusion, the 6-Myr-long astronomically-tuned timescale across OAE2 presented in this study allows for the evaluation and combination of two leading hypotheses about OAE2 forcing mechanisms.

Deleted: ongoing

Deleted: However,

Deleted: carbon cycle perturbations may

Deleted: was possibly responsible for observed

Acknowledgements

Special thanks go to the Association "Le montagne di San Francesco" for logistic support in the field, as well as the inhabitants of Coldigioco. We would like to thank Jiří Laurin and two anonymous reviewers for their feedback, as well as Stephen Meyers, Nicolas Thibault, Ian Jarvis, André Bornemann and an anonymous reviewer for comments on a previous version of the manuscript. DDV thanks the Research Foundation Flanders (FWO) for a Ph.D. scholarship and the EARTHSEQUENCING project (ERC Consolidator Grant). SJB thanks the European Community funded GTSnext project (grant agreement 215458), the European Science

Deleted: We would like to thank

Foundation activity ‘EARTHTIME—The European Contribution’ (Exchange Grant 3818) and the German Research Foundation (DFG VO 687/14-1, IODP/ODP SSP 527/32). PhC acknowledges the support of the Hercules foundation for upgrade of the VUB stable isotope laboratory.

References

Adams, D., Hurtgen, M., and Sageman, B.: Volcanic triggering of a biogeochemical cascade during Oceanic Anoxic Event 2, Nature Geoscience, 3 (3), 201-204, 2010.

Alvarez, W., Montanari, A., and Shimabukuro, D.: Ex Libro Lapidum Historia Mundi: Reading History Written in Rocks, in: Evolution: A Big History Perspective, edited by: Grinin, L. E., Korotayev, A. V., and Rodrigue, B. H., Uchitel Publishing House, Volgograd, 145-157, 2011.

Beaudouin, B., M'Ban, E. P., Montanari, A., and Pinault, M.: Lithostratigraphie haute résolution (< 20 ka) dans le Cénomanien du bassin d'Ombrie-Marches (Italie), Comptes rendus de l'Académie des sciences. Série 2. Sciences de la terre et des planètes 323 (8), 689-696, 1996.

Berger, A., Loutre, M. F., and Laskar, J.: Stability of the Astronomical Frequencies Over the Earth's History for Paleoclimate Studies, Science, 255 (5044), 560-566, 1992.

Caron, M., Dall'Agnolo, S., Accarie, H., Barrera, E., Kauffman, E., Amédro, F., and Robaszynski, F.: High-resolution stratigraphy of the Cenomanian–Turonian boundary interval at Pueblo (USA) and wadi Bahloul (Tunisia): stable isotope and bio-events correlation, Geobios, 39 (2), 171-200, 2006.

Cleveland, W. S.: Robust Locally Weighted Regression and Smoothing Scatterplots, Journal of the American Statistical Association, 74 (368), 829-836, 1979.

Coccioni, R., 1996. The Cretaceous of the Umbria–Marche Apennines (Central Italy). Jost Wiedmann Symposium "Cretaceous Stratigraphy, Paleobiology and Paleobiogeography", Tübingen, 7–10 March 1996, pp. 129–136, 1996.

de Boer, P. L.: Cyclicity and the Storage of Organic Matter in Middle Cretaceous Pelagic Sediments, in: Cyclic and Event Stratification, edited by: Einsele, G., and Seilacher, A., Springer Berlin Heidelberg, Berlin, Heidelberg, 456-475, 1982.

de Boer, P. L.: Aspects of middle cretaceous pelagic sedimentation in Southern Europe: production and storage of organic matter, stable isotopes, and astronomical influences, Geologica Ultraiectina, 31, 1-112, 1983.

Du Vivier, A., Selby, D., Sageman, B., Jarvis, I., Gröcke, D., and Voigt, S.: Marine $^{187}Os/^{188}Os$ isotope stratigraphy reveals the interaction of volcanism and ocean circulation during Oceanic Anoxic Event 2, Earth and Planetary Science Letters, 389, 23-33, 2014.

Eldrett, J. S., Ma, C., Bergman, S. C., Lutz, B., Gregory, F. J., Dodsworth, P., Phipps, M., Hardas, P., Minisini, D., Ozkan, A., Ramezani, J., Bowring, S. A., Kamo, S. L., Ferguson, K., Macaulay, C., and Kelly, A. E.: An astronomically calibrated stratigraphy of the Cenomanian, Turonian and earliest Coniacian from the Cretaceous Western Interior Seaway, USA: Implications for global chronostratigraphy, Cretaceous Research, 56, 316-344, 2015.

Gale, A., Voigt, S., Sageman, B., and Kennedy, W.: Eustatic sea-level record for the Cenomanian (Late Cretaceous)—extension to the Western Interior Basin, USA, Geology, 36 (11), 859-862, 2008.

Gambacorta, G., Jenkyns, H. C., Russo, F., Tsikos, H., Wilson, P. A., Faucher, G., and Erba, E.: Carbon- and oxygen-isotope records of mid-Cretaceous Tethyan pelagic sequences from the Umbria-Marche and Belluno Basins (Italy), Newsletters on Stratigraphy, 48, 299-323, 2015.

Giorgioni, M., Weissert, H., Bernasconi, S. M., Hochuli, P. A., Coccioni, R., and Keller, C. E.: Orbital control on carbon cycle and oceanography in the mid-Cretaceous greenhouse, Paleoceanography, 27 (1), 10.1029/2011PA002163, 2012.

Herbert, T. D., and Fischer, A. G.: Milankovitch climatic origin of mid-Cretaceous black shale rhythms in central Italy, Nature, 321, 739-743, 1986.

Hilgen, F., Aziz, H. A., Krijgsman, W., Raffi, I., and Turco, E.: Integrated stratigraphy and astronomical tuning of the Serravallian and lower Tortonian at Monte dei Corvi (Middle–Upper Miocene, northern Italy), Palaeogeography, Palaeoclimatology, Palaeoecology, 199 (3), 229-264, 2003.

Jarvis, I., Gale, A., Jenkyns, H., and Pearce, M.: Secular variation in Late Cretaceous carbon isotopes: a new $\delta^{13}C$ carbonate reference curve for the Cenomanian-Campanian (99.6-70.6 Ma), Geological Magazine, 143 (5), 561-608, 2006.

Jenkyns, H. C., Gale, A. S., and Corfield, R. M.: Carbon- and oxygen-isotope stratigraphy of the English Chalk and Italian Scaglia and its palaeoclimatic significance, Geological Magazine, 131 (1), 1-34, 1994.

Jenkyns, H. C., Matthews, A., Tsikos, H., and Erel, Y.: Nitrate reduction, sulfate reduction, and sedimentary iron isotope evolution during the Cenomanian-Turonian oceanic anoxic event, Paleoceanography, 22 (3), doi 10.1029/2006PA001355, 2007.

Kuiper, K., Deino, A., Hilgen, F., Krijgsman, W., Renne, P., and Wijbrans, J.: Synchronizing rock clocks of Earth history, Science, 320 (5875), 500-504, 2008.

Kuroda, J., Ogawa, N. O., Tanimizu, M., Coffin, M. F., Tokuyama, H., Kitazato, H., and Ohkouchi, N.: Contemporaneous massive subaerial volcanism and late cretaceous Oceanic Anoxic Event 2, Earth and Planetary Science Letters, 256 (1), 211-223, 2007.

Lanci, L., Muttoni, G., and Erba, E.: Astronomical tuning of the Cenomanian Scaglia Bianca Formation at Furlo, Italy, Earth and Planetary Science Letters, 292 (1), 231-237, 2010.

Laskar, J., Robutel, P., Joutel, F., Gastineau, M., Correia, A., and Levrard, B.: A long-term numerical solution for the insolation quantities of the Earth, Astronomy & Astrophysics, 428 (1), 261-285, 2004.

Laskar, J., Fienga, A., Gastineau, M., and Manche, H.: La2010: a new orbital solution for the long-term motion of the Earth, Astronomy & Astrophysics, 532, A89, 2011a.

Laskar, J., Gastineau, M., Delisle, J., Farrés, A., and Fienga, A.: Strong chaos induced by close encounters with Ceres and Vesta, Astronomy & Astrophysics, 532, L4, 2011b.

Laurin, J., Meyers, S., Uličný, D., Jarvis, I., and Sageman, B.: Axial obliquity control on the greenhouse carbon budget through middle- to high-latitude reservoirs, Paleoceanography, 30 (2), 133-149, 2015.

Laurin, J., Meyers, S. R., Galeotti, S., and Lanci, L.: Frequency modulation reveals the phasing of orbital eccentricity during Cretaceous Oceanic Anoxic Event II and the Eocene hyperthermals, Earth and Planetary Science Letters, 442, 143-156, 2016.

Leckie, R. M.: Foraminifera of the Cenomanian-Turonian boundary interval, Greenhorn Formation, Rock Canyon Anticline, Pueblo, Colorado, in: Fine-grained deposits and biofacies of the Cretaceous Western Interior Seaway: Evidence of cyclic sedimentary processess: SEPM Field Trip Guidebook No. 4, edited by: Pratt, L., Kauffman, E., and Zelt, F., 139-155, 1985.

Ma, C., Meyers, S. R., Sageman, B. B., Singer, B. S., and Jicha, B. R.: Testing the astronomical time scale for oceanic anoxic event 2, and its extension into Cenomanian strata of the Western Interior Basin (USA), Geological Society of America Bulletin, 126 (7-8), 974-989, 2014.

Martin, E. E., MacLeod, K. G., Berrocoso, A. J., and Bourbon, E.: Water mass circulation on Demerara Rise during the Late Cretaceous based on Nd isotopes, Earth and Planetary Science Letters, 327, 2012.

Meyers, S., and Sageman, B.: Quantification of deep-time orbital forcing by average spectral misfit, American Journal of Science, 307 (5), 773-792, 2007.

Meyers, S., Sageman, B., and Arthur, M.: Obliquity forcing of organic matter accumulation during Oceanic Anoxic Event 2, Paleoceanography, 27 (3), doi:10.1029/2012PA002286, 2012a.

Meyers, S., Siewert, S., Singer, B., Sageman, B., Condon, D., Obradovich, J., Jicha, B., and Sawyer, D.: Intercalibration of radioisotopic and astrochronologic time scales for the Cenomanian-Turonian boundary interval, Western Interior Basin, USA, Geology, 40 (1), 7-10, 2012b.

Meyers, S. R.: Seeing red in cyclic stratigraphy: Spectral noise estimation for astrochronology, Paleoceanography, 27 (3), doi:10.1029/2012PA002307, 2012.

Meyers, S. R.: Astrochron: An R Package for Astrochronology. http://cran.r-project.org/package=astrochron, 2014

Min, K., Mundil, R., Renne, P. R., and Ludwig, K. R.: A test for systematic errors in 40Ar/39Ar geochronology through comparison with U/Pb analysis of a 1.1-Ga rhyolite, Geochimica et Cosmochimica Acta, 64 (1), 73-98, 2000.

Mitchell, R., Bice, D., Montanari, A., Cleaveland, L., Christianson, K., Coccioni, R., and Hinnov, L.: Oceanic anoxic cycles? Orbital prelude to the Bonarelli Level (OAE 2), Earth and Planetary Science Letters, 267 (1), 1-16, 2008.

Montanari, A., Chan, L., and Alvarez, W.: Synsedimentary Tectonics in the Late Cretaceous Early Tertiary Pelagic Basin of the Northern Apennines, Italy, in: Controls on Carbonate Platform and Basin Development, edited by: Crevello, P. D., Wilson, J. L., Sarg, J. F., and Read, J. F., The Society of Economic Paleontologists and Mineralogists, Special Publication 44, 379-399, 1989.

Obradovich, J.: A Cretaceous time scale, in: Evolution of the Western Interior Basin, edited by: Caldzell, W. G. E., and Kauffman, E., Geological Association of Canada, 379-396, 1993.

Paillard, D., Labeyrie, L., and Yiou, P.: Macintosh program performs time-series analysis, Eos, Transactions American Geophysical Union, 77 (39), 379, 1996.

Reimold, W. U., Koeberl, C., and Bishop, J.: Roter Kamm impact crater, Namibia: Geochemistry of basement rocks and breccias, Geochimica et Cosmochimica Acta, 58 (12), 2689-2710, 1994.

Renne, P., Deino, A., Hilgen, F., Kuiper, K., Mark, D., Mitchell, W., Morgan, L., Mundil, R., and Smit, J.: Time Scales of Critical Events Around the Cretaceous-Paleogene Boundary, Science, 339 (6120), 2013.

Renne, P. R., Swisher, C. C., Deino, A. L., Karner, D. B., Owens, T. L., and DePaolo, D. J.: Intercalibration of standards, absolute ages and uncertainties in 40Ar/39Ar dating, Chemical Geology, 145 (1), 117-152, 1998.

Ruckstuhl, A. F., Jacobson, M. P., Field, R. W., and Dodd, J. A.: Baseline subtraction using robust local regression estimation, Journal of Quantitative Spectroscopy and Radiative Transfer, 68 (2), 179-193, 2001.

Sageman, B., Meyers, S., and Arthur, M.: Orbital time scale and new C-isotope record for Cenomanian-Turonian boundary stratotype, Geology, 34 (2), 125-128, 2006.

Sageman, B. B., Singer, B. S., Meyers, S. R., Siewert, S. E., Walaszczyk, I., Condon, D. J., Jicha, B. R., Obradovich, J. D., and Sawyer, D. A.: Integrating 40Ar/39Ar, U-Pb, and astronomical clocks in the Cretaceous Niobrara Formation, Western Interior Basin, USA, Geological Society of America Bulletin, 126 (7-8), 956-973, 2014.

Schwarzacher, W.: Cyclostratigraphy of the Cenomanian in the Gubbio district, Italy: a field study, in: Orbital forcing and cyclic sequences, edited by De Boer, P. L. and Smith, D. G., Blackwell Publishing Ltd., Oxford, 87-97, 1994.

Scopelliti, G., Bellanca, A., Neri, R., Baudin, F., and Coccioni, R.: Comparative high-resolution chemostratigraphy of the Bonarelli Level from the reference Bottaccione section (Umbria-Marche Apennines) and from an equivalent section in NW Sicily: Consistent and contrasting responses to the OAE2, Chemical Geology, 228 (4), 266-285, 2006.

Sinton, C., and Duncan, R.: Potential links between ocean plateau volcanism and global ocean anoxia at the Cenomanian-Turonian boundary, Economic Geology, 92 (7-8), 836-842, 1997.

Sissingh, W.: Biostratigraphy of Cretaceous calcareous nannoplankton, Geologie en mijnbouw, 56, 37-65, 1977.

Snow, L., Duncan, R., and Bralower, T.: Trace element abundances in the Rock Canyon Anticline, Pueblo, Colorado, marine sedimentary section and their relationship to Caribbean plateau construction and oxygen anoxic event 2, Paleoceanography, 20 (3), doi:10.1029/2004PA001093, 2005.

Sprovieri, M., Sabatino, N., Pelosi, N., Batenburg, S. J., Coccioni, R., Iavarone, M., and Mazzola, S.: Late Cretaceous orbitally-paced carbon isotope stratigraphy from the Bottaccione Gorge (Italy), Palaeogeography, Palaeoclimatology, Palaeoecology, 379–380, 81-94, 2013.

Stoll, H., and Schrag, D.: High-resolution stable isotope records from the Upper Cretaceous rocks of Italy and Spain: Glacial episodes in a greenhouse planet?, Geological Society of America Bulletin, 112 (2), 308-319, 2000.

Takashima, R., Nishi, H., Hayashi, K., Okada, H., Kawahata, H., Yamanaka, T., Fernando, A. G., and Mampuku, M.: Litho-, bio- and chemostratigraphy across the Cenomanian/Turonian boundary (OAE 2) in the Vocontian Basin of southeastern France, Palaeogeography, Palaeoclimatology, Palaeoecology, 273 (1), 61-74, 2009.

Thomson, D. J.: Spectrum Estimation and Harmonic-Analysis, Proceedings of the IEEE, 70 (9), 1055-1096, 1982.

Trabucho-Alexandre, J., Tuenter, E., Henstra, G., van der Zwan, K., van de Wal, R., Dijkstra, H., and de Boer, P.: The mid-Cretaceous North Atlantic nutrient trap: Black shales and OAEs, Paleoceanography, 25 (4), doi:10.1029/2010pa001925, 2010.

Trabucho-Alexandre, J., Negri, A., and de Boer, P. L.: Early Turonian pelagic sedimentation at Moria (Umbria-Marche, Italy): Primary and diagenetic controls on lithological oscillations, Palaeogeography, Palaeoclimatology, Palaeoecology, 311 (3), 200-214, 2011.

Tsikos, H., Jenkyns, H. C., Walsworth-Bell, B., Petrizzo, M. R., Forster, A., Kolonic, S., Erba, E., Silva, I. P., Baas, M., Wagner, T., and Damste, J. S. S.: Carbon-isotope stratigraphy recorded by the Cenomanian-Turonian Oceanic Anoxic Event: correlation and implications based on three key localities, Journal of the Geological Society, 161 (4), 711-719, 2004.

Turgeon, S., and Creaser, R.: Cretaceous oceanic anoxic event 2 triggered by a massive magmatic episode, Nature, 454 (7202), 323-326, 2008.

Voigt, S., Gale, A., and Voigt, T.: Sea-level change, carbon cycling and palaeoclimate during the Late Cenomanian of northwest Europe; an integrated palaeoenvironmental analysis, Cretaceous Research, 27 (6), 836-858, 2006.

Voigt, S., Erbacher, J., Mutterlose, J., Weiss, W., Westerhold, T., Wiese, F., Wilmsen, M., and Wonik, T.: The Cenomanian Turonian of the Wunstorf section (North Germany): global stratigraphic reference section and new orbital time scale for Oceanic Anoxic Event 2, Newsletters on Stratigraphy, 43 (1), 65-89, 2008.

Zachos, J. C., McCarren, H., Murphy, B., Röhl, U., and Westerhold, T.: Tempo and scale of late Paleocene and early Eocene carbon isotope cycles: Implications for the origin of hyperthermals, Earth and Planetary Science Letters, 299, 242-249, 2010.

Zheng, X.-Y., Jenkyns, H., Gale, A., Ward, D., and Henderson, G.: Changing ocean circulation and hydrothermal inputs during Ocean Anoxic Event 2 (Cenomanian–Turonian): evidence from Nd-isotopes in the European shelf sea, Earth and Planetary Science Letters, 375, 338-348, 2013.

Deleted: Adams, D., Hurtgen, M., and Sageman, B.: Volcanic triggering of a biogeochemical cascade during Oceanic Anoxic Event 2, Nat. Geosci., 3, 201-204, doi:10.1038/ngeo743, 2010. ... [6]

Table 1. Astronomical tuning options for biostratigraphic and isotopic events and comparison to radioisotopic ages. Uncertainties on tuned absolute ages comprise the uncertainty in the stratigraphic position and/or correlation of an event (± 0.75 m) and the uncertainty in the astronomical target curve (Laskar et al., 2011a) (± 0.079 Myr). The numerical age of the C/T boundary is based on intercalibration of $^{40}Ar/^{39}Ar$ dating, U-Pb dating and astrochronology (Meyers et al., 2012b); Radioisotopic age of the Base of *Whiteinella archaeocretacea* is the weighted mean age of single and multicrystal $^{40}Ar/^{39}Ar$ ages of bentonite A; Radioisotopic ages for the first peak of the Mid-Cenomanian event come from single crystal $^{40}Ar/^{39}Ar$ dating of the Thatcher bentonite in the *Conlinceras tarrantense* zone (Calycoceras *gilberti*). All radioisotopic ages are reported in 2σ and using a FC age of 28.201 ± 0.046 ka (1σ) (Kuiper et al., 2008).

Deleted: 46

Event	Stratigraphic Level (m)	Tuning #1 (Ma) with stratigraphic and astronomical uncertainty	Tuning #2 (Ma) with stratigraphic and astronomical uncertainty	Radioisotopic dating (Ma) with 2σ radiometric uncertainty
***Hitch Wood* $\delta^{13}C$ excursion**	516.24 m	90.59 ± 0.15	90.99 ± 0.15	
Base D. primitiva - M. sigali	508.85 m	91.31 ± 0.15	91.72 ± 0.15	
***Round down* $\delta^{13}C$ excursion**	499.44 m	92.32 ± 0.15	92.72 ± 0.15	
Base NC14	493.85 m	92.93 ± 0.15	93.33 ± 0.15	
Base *Helvetoglobotruncana helvetica*	491.85 m	93.17 ± 0.15	93.57 ± 0.15	
C/T boundary	487.47 m	93.69 ± 0.15	94.10 ± 0.15	93.90 ± 0.15 (Meyers et al., 2012b)
Base *Whiteinella archaeocretacea*	485.70 m	94.17 ± 0.15	94.57 ± 0.15	94.20 ± 0.28 (Meyers et al., 2012b)
Base NC12	484.20 m	94.28 ± 0.15	94.68 ± 0.15	
Base CC10	482.77 m	94.39 ± 0.15	94.79 ± 0.15	
first peak Mid-Cenomanian event	466.47 m	96.09 ± 0.15	96.49 ± 0.15	96.21 ± 0.36 this study

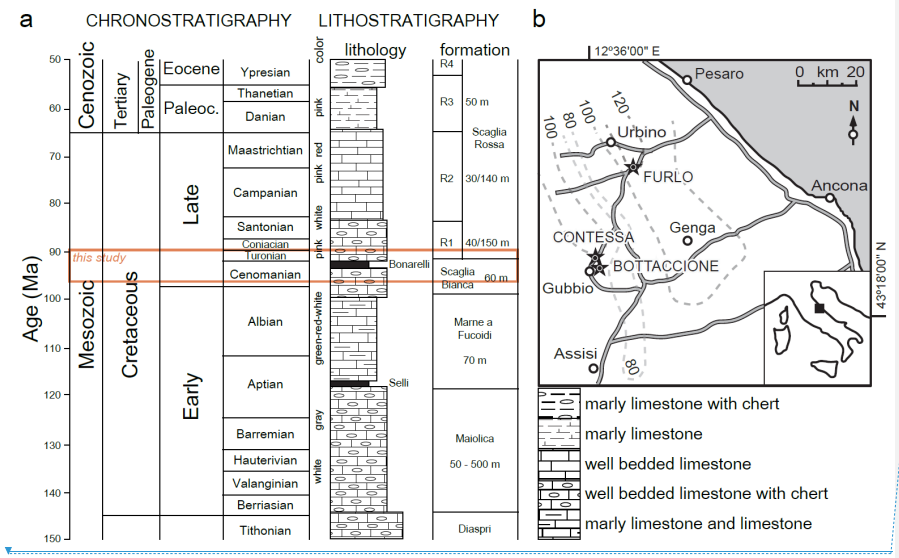

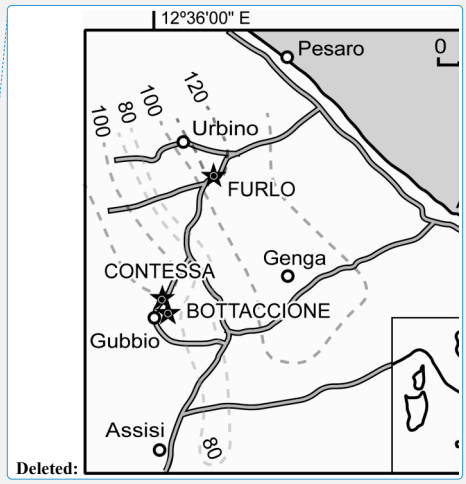

Deleted:

Figure 1. **(a)** Chrono- and lithostratigraphy of the Umbria-Marche succession in the Apennine mountains (adapted from Alvarez et al., 2011). **(b)** Geographic setting of the study sections with isopachs of the Bonarelli level (in cm) from Montanari et al.(1989).

Deleted: Figure 1. Geographic setting of the study sections with isopachs of the Bonarelli level (in cm) from Montanari et al.(1989).

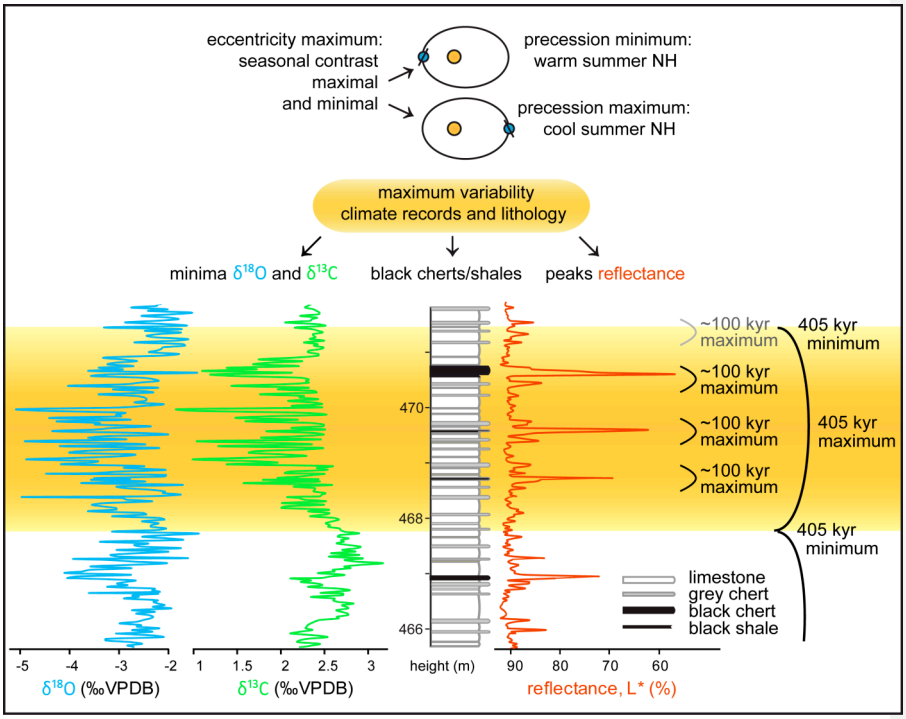

Figure 2. Phase relationship between eccentricity and proxy records. During eccentricity maxima, the seasonal contrast for the NH is maximally enhanced during precession minima and maximally reduced during precession maxima (top: schematic representation of the Earth's orbit around the sun). Hence, climate variability is strongly amplified during eccentricity maxima, triggering the highest variability in the climate-sensitive records and hierarchical organization of chert-limestone alternations.

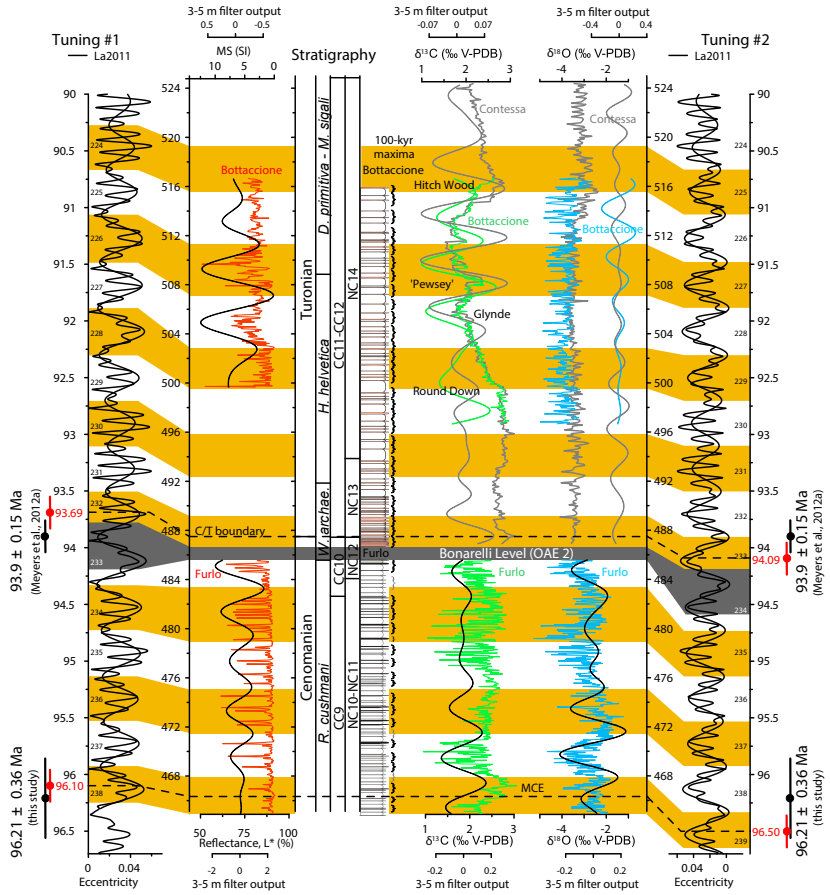

Figure 3. Cyclostratigraphic interpretation of the C/T interval of the Umbria-Marche basin. Brackets indicate 100-kyr bundles of precession-paced lithological alternations, further grouping in 405-kyr cycles is indicated by alternating yellow-white bands. Geophysical records (L* and MS) accentuate the hierarchical stacking pattern. Stable isotope ratios show increased amplitude and a tendency towards more negative values during eccentricity maxima. Isotopic records in grey are from Stoll and Schrag (2000). Event names in italics refer to nomenclature of Jarvis et al. (2006). Astronomical tuning options to La2011 are presented, with 405-kyr cycle numbering back from the present day, next to radioisotopic ages discussed in this study.

Deleted:

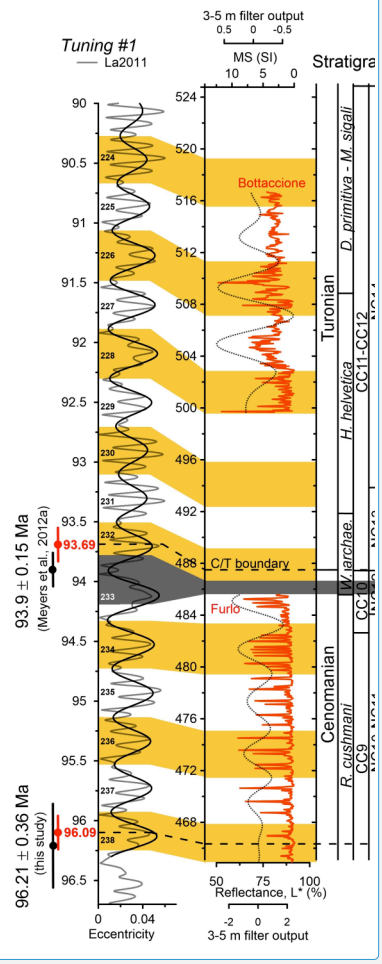

Deleted: Circumflexes

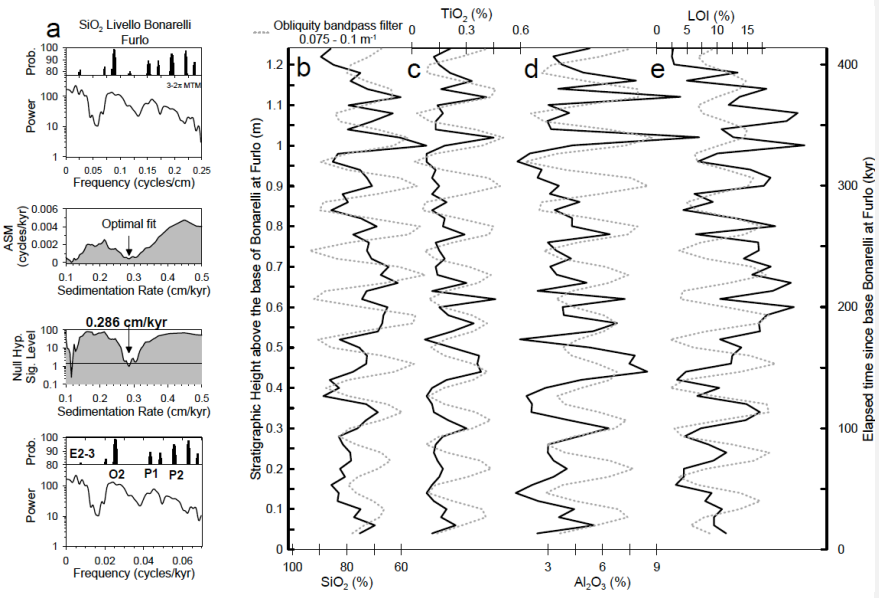

Figure 4. Duration estimate of Livello Bonarelli at Furlo based on **(a)** the Average Spectral Misfit (ASM) method. **(b-e)** SiO_2, TiO_2, and Al_2O_3 contents and Loss on Ignition (LOI) data show ~12-cm-thick cycles, interpreted as obliquity. The duration of Livello Bonarelli at Furlo is estimated at 413 kyr.

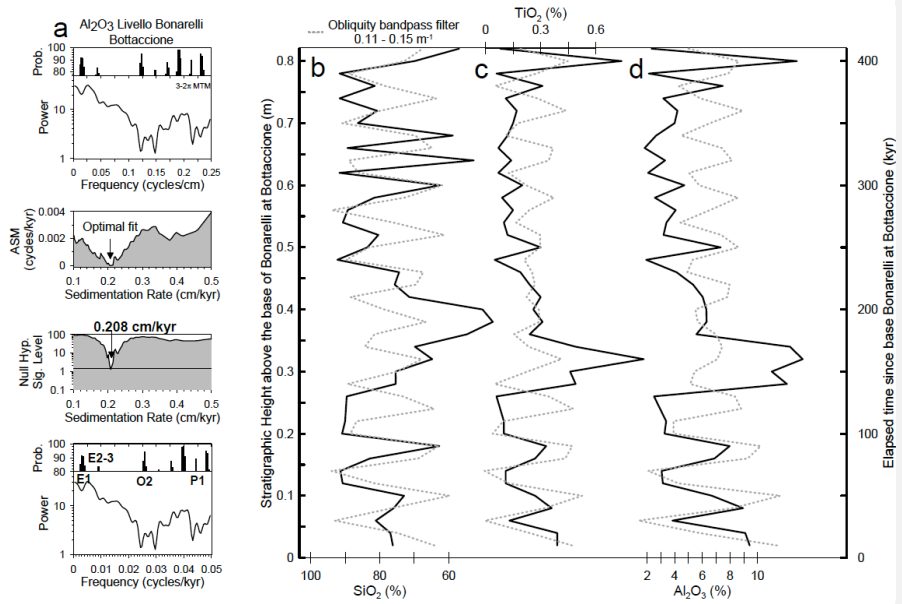

Figure 5. Duration estimate of Livello Bonarelli at Bottaccione based on (a) the Average Spectral Misfit (ASM) method. (b-d) SiO_2, TiO_2 and Al_2O_3 data show ~8-cm thick cycles, interpreted as obliquity. The duration of Livello Bonarelli at Bottaccione is estimated at 410 kyr.

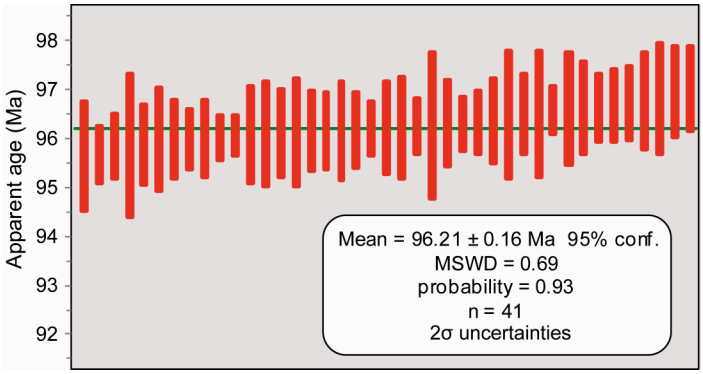

Figure 6. Summary of $^{40}Ar/^{39}Ar$ results

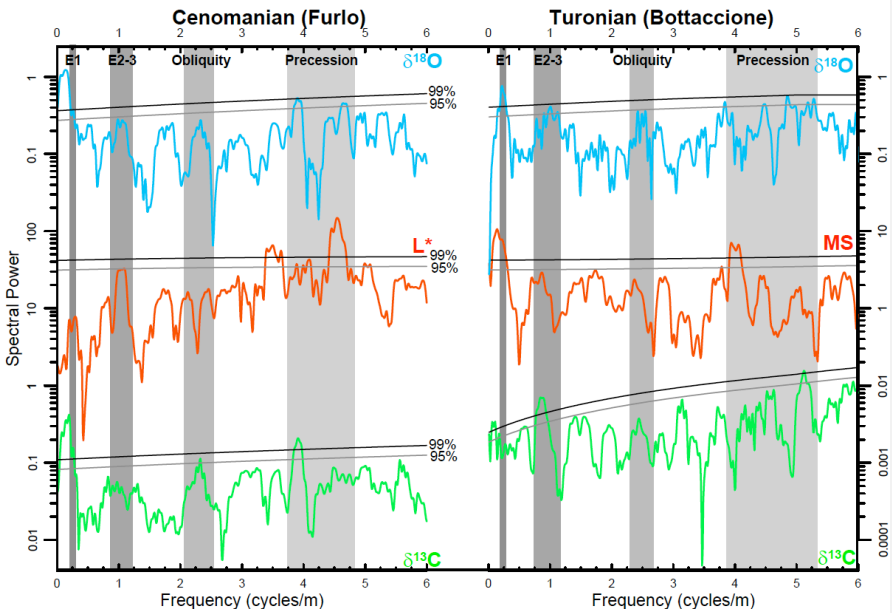

Figure 7. MTM/LOWSPEC spectra of proxy records. All proxy records show a strong imprint of eccentricity-modulated precession (E2-3: short eccentricity), $\delta^{13}C$ from Furlo also displays a statistically significant (>95% confidence level) imprint of obliquity.

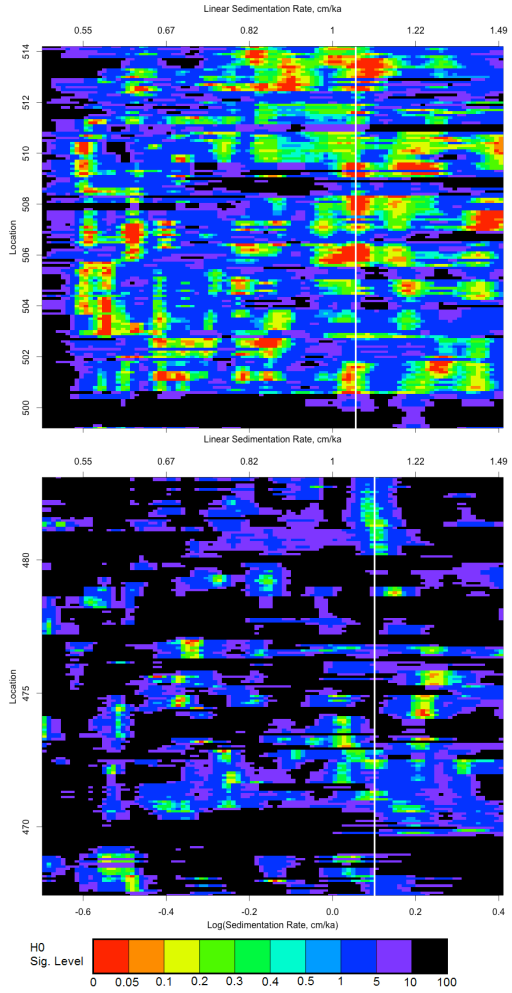

Figure 8. Evolutionary average spectral misfit (eASM) of the $\delta^{13}C$ data from Furlo (bottom) and Bottaccione (top), with a 5 m window, 0.1 m steps and using those frequencies with F-test > 80%. The white line suggests a stable sedimentation rate of 1.1 cm/kyr in Furlo and 1.05 cm/kyr in Bottaccione.

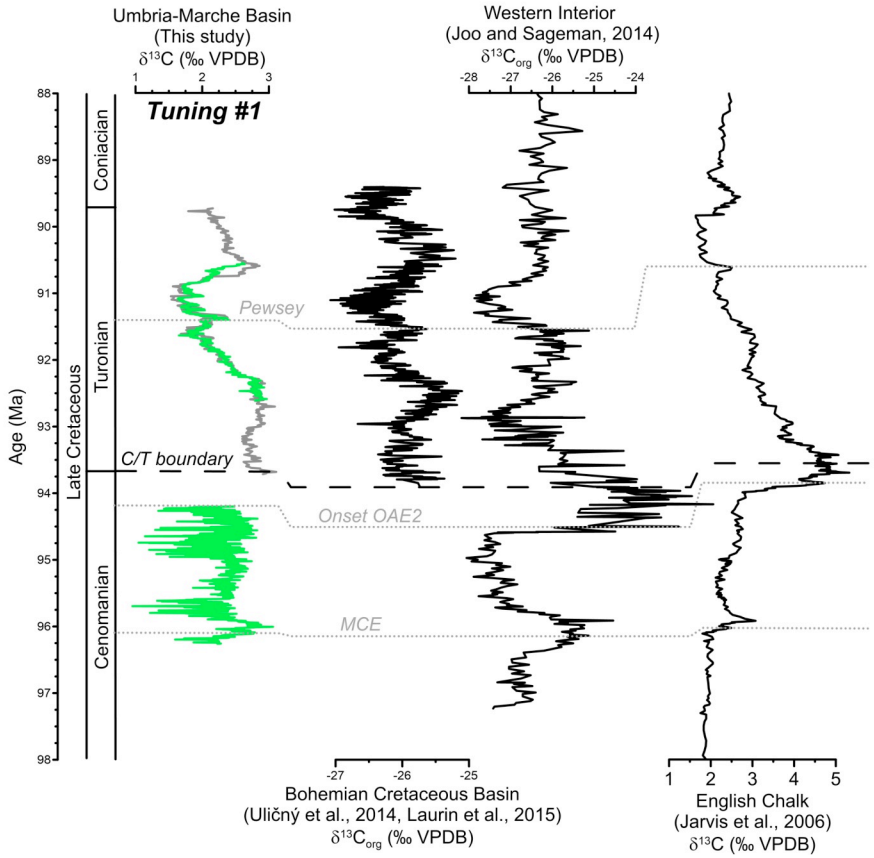

Figure 9. Global correlation of $\delta^{13}C_{carb}$ data of the Cenomanian-Turonian interval.

Page 9: [1] Deleted authors 8/1/16 6:05:00 PM

Stable isotopes and diagenesis

The records of $\delta^{18}O$ and $\delta^{13}C$ show long-term trends over the successions, although the $\delta^{18}O$ record in particular displays scatter which might be due to an influence of diagenesis. $\delta^{13}C$ is generally more robust to post-depositional alteration (Jenkyns et al., 1994) and bulk carbonate $\delta^{13}C$ patterns have been shown to be a powerful tool for stratigraphic correlation, despite variations in absolute values and amplitude amongst locations (Jarvis et al., 2006). Although variability at the sampling scale (3 cm) may partially represent effects of diagenesis which could obscure short (precessional scale) climatic signals, the longer term trends compare well with coeval sections in the Umbria-Marche basin (Stoll and Schrag, 2000; Sprovieri et al., 2013) and the English chalk records (Jarvis et al., 2006) (Figure 9).

Page 11: [2] Deleted authors 8/1/16 6:05:00 PM

Anchoring the Astrochronology

Correlation of the C/T boundary

In this study, the base of the Turonian stage at Bottaccione is placed at 487.47 m, just above the first occurrence of *Quadrum gartneri* at 487.25 m defining the base of the C11 zone (Sissingh, 1977), following Sprovieri et al. (2013) and Tsikos et al.

1.1.1

Page 11: [3] Deleted authors 8/1/16 6:05:00 PM

Tuning options

Because of its stability, only the 405-kyr component of eccentricity can be used for astronomical tuning in the Cretaceous and not the ~100 kyr periodicity that was used in previous tuning efforts (Mitchell et al., 2008). The shorter obliquity and precession terms can only be used for the development of floating time scales.

Page 13: [4] Deleted authors 8/1/16 6:05:00 PM

Radioisotopic dating

Page 15: [5] Deleted authors 8/1/16 6:05:00 PM

The new astrochronologies allow for assessing the long-term behavior of the carbon cycle during the C/T transition. The onset of the MCE, the base of the Livello Bonarelli, and the middle of the negative $\delta^{13}C$ excursion of the mid-Turonian are separated by 2.0 Myr and 2.4 Myr, respectively. The 1.6 Myr long negative excursion in the mid-Turonian is characterized by an intermittent double positive peak ("Pewsey events"; Jarvis et al., 2006), similar to the MCE, starting at 91.7 Ma (tuning #1) or 92.1 Ma (tuning #2). These repetitive variations in $\delta^{13}C$, superimposed on the long-term behavior of the carbon cycle, are likely paced by the ~2.4-Myr eccentricity period. Following tuning #1, a tentative comparison with the full eccentricity solution La2011 (Fig. 2) reveals the occurrence of pronounced long-term minima in eccentricity before the mid-Cenomanian and mid-Turonian events.

Trace element studies indicate that volcanic activity of the Caribbean Large Igneous Province increasingly supplied nutrients and sulphate to a low-sulphate ocean, with a major pulse ~500 kyr before OAE2 (Snow et al., 2005; Jenkyns et al., 2007; Turgeon and Creaser, 2008; Adams et al., 2010). This is manifested

Page 22: [6] Deleted authors 8/1/16 6:05:00 PM

Adams, D., Hurtgen, M., and Sageman, B.: Volcanic triggering of a biogeochemical cascade during Oceanic Anoxic Event 2, Nat. Geosci., 3, 201-204, doi:10.1038/ngeo743, 2010.

Berger, A., Loutre, M. F., and Laskar, J.: Stability of the Astronomical Frequencies Over the Earth's History for Paleoclimate Studies, 255, 560-566, 10.1126/science.255.5044.560, 1992.

Caron, M., Dall'Agnolo, S., Accarie, H., Barrera, E., Kauffman, E., Amédro, F., and Robaszynski, F.: High-resolution stratigraphy of the Cenomanian–Turonian boundary interval at Pueblo (USA) and wadi Bahloul (Tunisia): stable isotope and bio-events correlation, Geobios, 39, 171-200, doi:10.1016/j.geobios.2004.11.004, 2006.

Cleveland, W. S.: Robust Locally Weighted Regression and Smoothing Scatterplots, J. Amer. Statist. Assoc., 74, 829-836, doi:10.1080/01621459.1979.10481038, 1979.

Coccioni, R.: The Cretaceous of the Umbria-Marche Apennines (central Italy), Wiedmann Symposium bCretaceous Stratigraphy, Paleobiology and PaleobiogeographyQ, the Umbria–Marche Apennines (Central Italy). Tübingen, 1996, 7-10,

Du Vivier, A., Selby, D., Sageman, B., Jarvis, I., Gröcke, D., and Voigt, S.: Marine $^{187}Os/^{188}Os$ isotope stratigraphy reveals the interaction of volcanism and ocean circulation during

Oceanic Anoxic Event 2, Earth Planet. Sci. Lett., 389, 23-33, doi:10.1016/j.epsl.2013.12.024, 2014.

Gale, A., Kennedy, W., Voigt, S., and Walaszczyk, I.: Stratigraphy of the Upper Cenomanian–Lower Turonian Chalk succession at Eastbourne, Sussex, UK: ammonites, inoceramid bivalves and stable carbon isotopes, Cretaceous Res., 26, 460-487, doi:10.1016/j.cretres.2005.01.006, 2005.

Gale, A., Voigt, S., Sageman, B., and Kennedy, W.: Eustatic sea-level record for the Cenomanian (Late Cretaceous)—extension to the Western Interior Basin, USA, Geology, 36, 859-862, doi:10.1130/G24838A.1, 2008.

Hilgen, F., Aziz, H. A., Krijgsman, W., Raffi, I., and Turco, E.: Integrated stratigraphy and astronomical tuning of the Serravallian and lower Tortonian at Monte dei Corvi (Middle–Upper Miocene, northern Italy), Palaeogeogr. Palaeocl., 199, 229-264, doi:10.1016/S0031-0182(03)00505-4, 2003.

Jarvis, I., Gale, A., Jenkyns, H., and Pearce, M.: Secular variation in Late Cretaceous carbon isotopes: a new $\delta^{13}C$ carbonate reference curve for the Cenomanian-Campanian (99.6-70.6 Ma), 143, 561-608, 2006.

Jenkyns, H. C., Gale, A. S., and Corfield, R. M.: Carbon- and oxygen-isotope stratigraphy of the English Chalk and Italian Scaglia and its palaeoclimatic significance, Geological Magazine, 131, 1-34, doi:10.1017/S0016756800010451, 1994.

Jenkyns, H. C., Matthews, A., Tsikos, H., and Erel, Y.: Nitrate reduction, sulfate reduction, and sedimentary iron isotope evolution during the Cenomanian-Turonian oceanic anoxic event, Paleoceanography, 22, PA3208, doi:10.1029/2006PA001355, 2007.

Kuiper, K., Deino, A., Hilgen, F., Krijgsman, W., Renne, P., and Wijbrans, J.: Synchronizing rock clocks of Earth history, Science, 320, 500-504, doi:10.1126/science.1154339, 2008.

Kuroda, J., Ogawa, N. O., Tanimizu, M., Coffin, M. F., Tokuyama, H., Kitazato, H., and Ohkouchi, N.: Contemporaneous massive subaerial volcanism and late cretaceous Oceanic Anoxic Event 2, Earth Planet Sc Lett, 256, 211-223, DOI 10.1016/j.epsl.2007.01.027, 2007.

Lanci, L., Muttoni, G., and Erba, E.: Astronomical tuning of the Cenomanian Scaglia Bianca Formation at Furlo, Italy, Earth Planet. Sci. Lett., 292, 231-237, doi:10.1016/j.epsl.2010.01.041, 2010.

Laskar, J., Fienga, A., Gastineau, M., and Manche, H.: La2010: a new orbital solution for the long-term motion of the Earth, Astron. Astrophys., 532, doi:10.1051/0004-6361/201116836, 2011a.

Laskar, J., Gastineau, M., Delisle, J., Farrés, A., and Fienga, A.: Strong chaos induced by close encounters with Ceres and Vesta., Astron. Astrophys., 532, 1-4, doi:10.1051/0004-6361/201117504 2011b.

Laurin, J., Meyers, S., Uličný, D., Jarvis, I., and Sageman, B.: Axial obliquity control on the greenhouse carbon budget through middle- to high-latitude reservoirs, 30, 133-149, 10.1002/2014PA002736, 2015.

Leckie, R. M.: Foraminifera of the Cenomanian-Turonian boundary interval, Greenhorn Formation, Rock Canyon Anticline, Pueblo, Colorado, in: Fine-grained deposits and biofacies of the Cretaceous Western Interior Seaway: Evidence of cyclic sedimentary

processess: SEPM Field Trip Guidebook No. 4, edited by: Pratt, L., Kauffman, E., and Zelt, F., 139-155, 1985.

Ma, C., Meyers, S. R., Sageman, B. B., Singer, B. S., and Jicha, B. R.: Testing the astronomical time scale for oceanic anoxic event 2, and its extension into Cenomanian strata of the Western Interior Basin (USA), Geol. Soc. Am. Bull., doi:10.1130/b30922.1, 2014.

Meyers, S., and Sageman, B.: Quantification of deep-time orbital forcing by average spectral misfit, Am. J. Sci., 307, 773-792, doi:10.2475/05.2007.01, 2007.

Meyers, S., Sageman, B., and Arthur, M.: Obliquity forcing of organic matter accumulation during Oceanic Anoxic Event 2, Paleoceanography, 27, PA3212, doi:10.1029/2012PA002286, 2012a.

Meyers, S., Siewert, S., Singer, B., Sageman, B., Condon, D., Obradovich, J., Jicha, B., and Sawyer, D.: Intercalibration of radioisotopic and astrochronologic time scales for the Cenomanian-Turonian boundary interval, Western Interior Basin, USA, Geology, 40, 7-10, doi:10.1130/G32261.1, 2012b.

Meyers, S. R.: Seeing red in cyclic stratigraphy: Spectral noise estimation for astrochronology, Paleoceanography, 27, PA3228, doi:10.1029/2012PA002307, 2012.

Min, K., Mundil, R., Renne, P. R., and Ludwig, K. R.: A test for systematic errors in 40Ar/39Ar geochronology through comparison with U/Pb analysis of a 1.1-Ga rhyolite, Geochim. Cosmochim. Ac. , 64, 73-98, doi:10.1016/S0016-7037(99)00204-5, 2000.

Mitchell, R., Bice, D., Montanari, A., Cleaveland, L., Christianson, K., Coccioni, R., and Hinnov, L.: Oceanic anoxic cycles? Orbital prelude to the Bonarelli Level (OAE 2), Earth. Planet. Sc. Lett., 267, 1-16, doi:10.1016/j.epsl.2007.11.026, 2008.

Montanari, A., Chan, L., and Alvarez, W.: Synsedimentary Tectonics in the Late Cretaceous Early Tertiary Pelagic Basin of the Northern Apennines, Italy, in: Soc Econ Pa, edited by: Crevello, P. D., Wilson, J. L., Sarg, J. F., and Read, J. F., The Society of Economic Paleontologists and Mineralogists, 379-399, 1989.

Obradovich, J.: A Cretaceous time scale, in: Evolution of the Western Interior Basin, edited by: Caldzell, W. G. E., and Kauffman, E., Geological Association of Canada, 379-396, 1993.

Paillard, D., Labeyrie, L., and Yiou, P.: Macintosh program performs time-series analysis, Eos Trans. A. G. U., 77, 379, 1996.

Reimold, W. U., Koeberl, C., and Bishop, J.: Roter Kamm impact crater, Namibia: Geochemistry of basement rocks and breccias, Geochim. Cosmochim. Ac., 58, 2689-2710, doi:10.1016/0016-7037(94)90138-4, 1994.

Renne, P., Deino, A., Hilgen, F., Kuiper, K., Mark, D., Mitchell, W., Morgan, L., Mundil, R., and Smit, J.: Time Scales of Critical Events Around the Cretaceous-Paleogene Boundary, Science, 339, 684-687, doi:10.1126/science.1230492 2013.

Ruckstuhl, A. F., Jacobson, M. P., Field, R. W., and Dodd, J. A.: Baseline subtraction using robust local regression estimation, J. Quant. Spectrosc. Ra., 68, 179-193, doi:10.1016/S0022-4073(00)00021-2, 2001.

Sageman, B., Meyers, S., and Arthur, M.: Orbital time scale and new C-isotope record for Cenomanian-Turonian boundary stratotype, Geology, 34, 125-128, doi:10.1130/G22074.1, 2006.

Sageman, B. B., Singer, B. S., Meyers, S. R., Siewert, S. E., Walaszczyk, I., Condon, D. J., Jicha, B. R., Obradovich, J. D., and Sawyer, D. A.: Integrating 40Ar/39Ar, U-Pb, and astronomical clocks in the Cretaceous Niobrara Formation, Western Interior Basin, USA, Geol. Soc. Am. Bull., 126, 956-973, doi:10.1130/b30929.1, 2014.

Scopelliti, G., Bellanca, A., Neri, R., Baudin, F., and Coccioni, R.: Comparative high-resolution chemostratigraphy of the Bonarelli Level from the reference Bottaccione section (Umbria-Marche Apennines) and from an equivalent section in NW Sicily: Consistent and contrasting responses to the OAE2, Chem. Geol., 228, 266-285, doi:10.1016/j.chemgeo.2005.10.010, 2006.

Sinton, C., and Duncan, R.: Potential links between ocean plateau volcanism and global ocean anoxia at the Cenomanian-Turonian boundary, Econ. Geol. Bull. Soc., 92, 836-842, doi:10.2113/gsecongeo.92.7-8.836 1997.

Sissingh, W.: Biostratigraphy of Cretaceous calcareous nannoplankton, Geol. Mijnbouw, 56, 37-65, 1977.

Snow, L., Duncan, R., and Bralower, T.: Trace element abundances in the Rock Canyon Anticline, Pueblo, Colorado, marine sedimentary section and their relationship to Caribbean plateau construction and oxygen anoxic event 2, Paleoceanography, 20, PA3005, doi:10.1029/2004PA001093, 2005.

Sprovieri, M., Sabatino, N., Pelosi, N., Batenburg, S. J., Coccioni, R., Iavarone, M., and Mazzola, S.: Late Cretaceous orbitally-paced carbon isotope stratigraphy from the Bottaccione Gorge (Italy), Palaeogeogr. Palaeocl., 379–380, 81-94, doi:10.1016/j.palaeo.2013.04.006, 2013.

Stoll, H., and Schrag, D.: High-resolution stable isotope records from the Upper Cretaceous rocks of Italy and Spain: Glacial episodes in a greenhouse planet?, Geol. Soc. Am. Bull., 112, 308-319, doi:10.1130/0016-7606, 2000.

Stoll, H. M., and Schrag, D. P.: Sr/Ca variations in Cretaceous carbonates: relation to productivity and sea level changes, Palaeogeogr. Palaeocl., 168, 311-336, doi:10.1016/S0031-0182(01)00205-X, 2001.

Takashima, R., Nishi, H., Hayashi, K., Okada, H., Kawahata, H., Yamanaka, T., Fernando, A. G., and Mampuku, M.: Litho-, bio- and chemostratigraphy across the Cenomanian/Turonian boundary (OAE 2) in the Vocontian Basin of southeastern France, Palaeogeogr. Palaeocl., 273, 61-74, doi:10.1016/j.palaeo.2008.12.001, 2009.

Thomson, D. J.: Spectrum Estimation and Harmonic-Analysis, P. IEEE, 70, 1055-1096, doi:10.1109/PROC.1982.12433, 1982.

Trabucho-Alexandre, J., Tuenter, E., Henstra, G., van der Zwan, K., van de Wal, R., Dijkstra, H., and de Boer, P.: The mid-Cretaceous North Atlantic nutrient trap: Black shales and OAEs, Paleoceanography, 25, PA4201, doi:10.1029/2010pa001925, 2010.

Trabucho-Alexandre, J., Negri, A., and de Boer, P. L.: Early Turonian pelagic sedimentation at Moria (Umbria-Marche, Italy): Primary and diagenetic controls on lithological oscillations, Palaeogeogr. Palaeocl., 311, 200-214, doi:10.1016/j.palaeo.2011.08.021, 2011.

Tsikos, H., Jenkyns, H. C., Walsworth-Bell, B., Petrizzo, M. R., Forster, A., Kolonic, S., Erba, E., Silva, I. P., Baas, M., Wagner, T., and Damste, J. S. S.: Carbon-isotope stratigraphy recorded by the Cenomanian-Turonian Oceanic Anoxic Event: correlation and implications based on three key localities, J Geol Soc London, 161, 711-719, 2004.

Turgeon, S., and Creaser, R.: Cretaceous oceanic anoxic event 2 triggered by a massive magmatic episode, Nature, 454, 323-326, doi:10.1038/nature07076, 2008.

Voigt, S., Gale, A., and Voigt, T.: Sea-level change, carbon cycling and palaeoclimate during the Late Cenomanian of northwest Europe; an integrated palaeoenvironmental analysis, Cretaceous Res., 27, 836-858, doi:10.1016/j.cretres.2006.04.005, 2006.

Voigt, S., Erbacher, J., Mutterlose, J., Weiss, W., Westerhold, T., Wiese, F., Wilmsen, M., and Wonik, T.: The Cenomanian Turonian of the Wunstorf section (North Germany): global stratigraphic reference section and new orbital time scale for Oceanic Anoxic Event 2, Newsl Stratigr, 43, 65-89, doi:10.1127/0078-0421/2008/0043-0065, 2008.

Zachos, J. C., McCarren, H., Murphy, B., Röhl, U., and Westerhold, T.: Tempo and scale of late Paleocene and early Eocene carbon isotope cycles: Implications for the origin of hyperthermals, Earth Planet. Sc. Lett, 299, 242-249, doi:10.1016/j.epsl.2010.09.004, 2010.

Zheng, X.-Y., Jenkyns, H., Gale, A., Ward, D., and Henderson, G.: Changing ocean circulation and hydrothermal inputs during Ocean Anoxic Event 2 (Cenomanian–Turonian): evidence from Nd-isotopes in the European shelf sea, Earth Planet. Sc. Lett., 375, 338-348, doi:10.1016/j.epsl.2013.05.053, 2013.